

1 ***Plasmodium vinckei* genomes provide insights into the**
2 **pan-genome and evolution of rodent malaria parasites**

3

4 Abhinay Ramaprasad ^{1,2,6}, Severina Klaus ^{2,3}, Olga Douvropoulou ¹, Richard
5 Culleton ^{2,4*} and Arnab Pain ^{1,5*}

6 ¹ Pathogen Genomics Group, BESE Division, King Abdullah University of Science
7 and Technology (KAUST), Thuwal 23955-6900, Kingdom of Saudi Arabia

8 ² Malaria Unit, Department of Pathology, Institute of Tropical Medicine (NEKKEN),
9 Nagasaki University, 1-12-4 Sakamoto, Nagasaki 852-8523, Japan

10 ³ Biomedical Sciences, University of Heidelberg, Heidelberg, Germany

11 ⁴ Division of Molecular Parasitology, Proteo-Science Center, Ehime University, 454
12 Shitsukawa, Toon, Ehime 791-0295, Japan

13 ⁵ Center for Zoonosis Control, Global Institution for Collaborative Research and
14 Education (GI-CoRE), Hokkaido University, N20 W10 Kita-ku, Sapporo 001-0020,
15 Japan

16 ⁶ Present address: Malaria Biochemistry Laboratory, Francis Crick Institute, London
17 NW1 1AT, UK

18 *arnab.pain@kaust.edu.sa, culleton.richard.oe@ehime-u.ac.jp

19

20

21

22

23

24

25

26 **Abstract**

27 **Background**

28 Rodent malaria parasites (RMPs) serve as tractable tools to study malaria parasite
29 biology and host-parasite-vector interactions. *Plasmodium vinckei* is the most
30 geographically widespread of the four RMP species collected in sub-Saharan Central
31 Africa. Several *P. vinckei* isolates are available but relatively less characterized than
32 other RMPs, thus hindering their use in experimental studies. We have generated a
33 comprehensive resource for *P. vinckei* comprising of high-quality reference
34 genomes, genotypes, gene expression profiles and growth phenotypes for ten *P.*
35 *vinckei* isolates.

36

37 **Results**

38 The *P. vinckei* subspecies have diverged widely from their common ancestor and
39 have undergone genomic structural variations. The subspecies from Katanga, *P. v.*
40 *vinckei*, has a uniquely smaller genome, a reduced multigene family repertoire and is
41 also amenable to genetic manipulation making it an ideal parasite for reverse
42 genetics. Comparing *P. vinckei* genotypes reveals region-specific selection
43 pressures particularly on genes involved in mosquito transmission. The erythrocyte
44 membrane antigen 1 and *fam-c* families have expanded considerably among the
45 lowland forest-dwelling *P. vinckei* parasites. Genetic crosses can be established in
46 *P. vinckei* but are limited at present by low transmission success under the
47 experimental conditions tested in this study.

48

49 **Conclusions**

50 *Plasmodium vinckei* isolates display a large degree of phenotypic and genotypic
51 diversity and could serve as a resource to study parasite virulence and
52 immunogenicity. Inclusion of *P. vinckei* genomes provide new insights into the
53 evolution of RMPs and their multigene families. Amenability to genetic crossing and
54 genetic manipulation make them also suitable for classical and functional genetics to
55 study *Plasmodium* biology.

56

57 **Keywords**

58 *Plasmodium vinckei*, Malaria, Rodent malaria parasites, Genomics, Transcriptomics,
59 Genetics, Parasite evolution, Multigene families

60

61 **Background**

62 Rodent malaria parasites (RMPs) serve as tractable models for experimental
63 genetics and as valuable tools to study malaria parasite biology and host-parasite-
64 vector interactions [1-4]. Between 1948 and 1974, several rodent malaria parasites
65 were isolated from wild thicket rats (shining thicket rat - *Grammomys poensis* or
66 previously known as *Thamnomys rutilans*, and woodland thicket rat - *Grammomys*
67 *surdaster*) and infected mosquitoes in sub-Saharan Africa and were adapted to
68 laboratory-bred mice and mosquitoes. The isolates were classified into four species,
69 namely, *Plasmodium berghei*, *Plasmodium yoelii*, *Plasmodium chabaudi* and
70 *Plasmodium vinckei*. *Plasmodium berghei* and *P. yoelii* are sister species forming the
71 classical *berghei* group, whereas *P. chabaudi* and *P. vinckei* form the classical
72 *vinckei* group of RMPs [5-7]. *Plasmodium chabaudi* has been used for studying drug
73 resistance, host immunity and immunopathology in malaria [8-12]. *Plasmodium yoelii*
74 and *P. berghei* are extensively used as tractable models to study liver and mosquito

75 stages of the parasite [13, 14]. Efficient transfection techniques [15-18] have been
76 established in all three RMPs and they are widely used as *in vivo* model systems for
77 large scale functional studies [19-22]. Reference genomes for these three RMP
78 species are available [23, 24]. Recently, the quality of these genomes has been
79 significantly improved using next-generation sequencing [11, 25, 26].

80

81 *P. vinckei* is the most geographically widespread RMP species, with isolates
82 collected from many locations in sub-Saharan Africa (Figure 1A). Subspecies
83 classifications were made for 18 *P. vinckei* isolates in total based on parasite
84 characteristics and geographical origin, giving rise to five subspecies; *P. v. vinckei*
85 (Democratic Republic of Congo), *P. v. petteri* (Central African Republic), *P. v. lentum*
86 (Congo Brazzaville), *P. v. brucechwatti* (Nigeria) and *P. v. subsp.* (Cameroon) [27-
87 32]. Blood, exo-erythrocytic and sporogonic stages of a limited number of isolates of
88 the five subspecies have been characterized; *P. v. vinckei* line 67 or CY [33], *P. v.*
89 *petteri* line CE [28], *P. v. lentum* line ZZ [29, 31], *P. v. brucechwatti* line 1/69 or DA
90 [30, 34] and several parasite lines of *P. v. subsp.* [35]. Enzyme variation studies [5,
91 36] and multi-locus sequencing data [6, 7] have indicated that there is significant
92 phenotypic and genotypic variation among *P. vinckei* isolates.

93 The rodent malaria parasites isolated from Cameroon in 1974 by J. M. Bafort are
94 currently without subspecies names, being designated as *P. yoelii subsp.*, *P. vinckei*
95 *subsp.* and *P. chabaudi subsp.*. We now present the full genome sequence data of
96 isolates from these subspecies and show they form distinct clades within their parent
97 species. Therefore, we propose the following subspecies names; *Plasmodium yoelii*
98 *cameronensis*, from the country of origin; *Plasmodium vinckei baforti*, after J. M.
99 Bafort, the original collector of this subspecies; and *Plasmodium chabaudi*

100 *esekanensis*, from Eséka, Cameroon, the town from the outskirts of which it was
101 originally collected.

102

103 Very few studies have employed *P. vinckei* compared to the other RMP species
104 despite the public availability of several *P. vinckei* isolates
105 (<http://www.malariaresearch.eu/content/rodent-malaria-parasites>). *Plasmodium v.*
106 *vinckei* v52 and *P. v. petteri* CR have been used to study parasite recrudescence
107 [37], chronobiology [38] and artemisinin resistance [39]. They are also the only
108 isolates for which draft genome assemblies with annotation are available as part of
109 the Broad Institute *Plasmodium* 100 Genomes initiative
110 (<https://www.ncbi.nlm.nih.gov/bioproject/163123>).

111

112 A high-quality reference genome for *P. vinckei* and detailed phenotypic and
113 genotypic data are lacking for the majority of *P. vinckei* isolates hindering wide-scale
114 adoption of this RMP species in experimental malaria studies.

115

116 We now present a comprehensive genome resource for *P. vinckei* comprising of
117 high-quality reference genomes for five *P. vinckei* isolates (one from each
118 subspecies) and describe the genotypic diversity within the *P. vinckei* clade through
119 the sequencing of five additional *P. vinckei* isolates (see Figure 1A inset). With the
120 aid of high-quality annotated genome assemblies and gene expression data, we
121 evaluate the evolutionary patterns of multigene families across all RMPs and within
122 the subspecies of *P. vinckei*.

123

124 We also describe the growth and virulence phenotypes of these isolates and show
125 that *P. vinckei* is amenable to genetic manipulation and can be used to generate
126 experimental genetic crosses.

127

128 Furthermore, we sequenced the whole genomes of seven isolates of the subspecies
129 of *P. chabaudi* (*P. c. esekanensis*) and *P. yoelii* (*P. y. yoelii*, *P. y. nigeriensis*, *P. y.*
130 *killicki* and *P. y. cameronensis*) in order to resolve evolutionary relationships among
131 RMP isolates.

132

133 The data presented here enable the use of the *P. vinckei* clade of parasites for
134 laboratory-based experiments driven by high-throughput genomics technologies and
135 will significantly expand the number of RMPs available as experimental models to
136 understand the biology of malaria parasites.

137

138 **Results**

139 ***Plasmodium vinckei* isolates display extensive diversity in virulence**

140 We followed the infection profiles of ten *P. vinckei* isolates in CBA/J mice (five
141 biological replicates per group) to study their virulence traits. Some of these isolates
142 were available as uncloned lines and so were first cloned by limiting dilution
143 (Additional File 1). As reported previously [40], *P. vinckei* parasites are
144 morphologically indistinguishable from each other, prefer to invade mature
145 erythrocytes, are largely synchronous during blood stage growth and display a
146 characteristically rich abundance of haemozoin crystals in their trophozoites and
147 gametocytes (Figure 1B).

148

149 Parasitaemia was determined daily to measure the growth rate of each isolate and
150 host RBC density and weight were measured as indications of “virulence” (harm
151 to the host) (Figure 1C, Additional file 2 and 3).

152

153 The *P. v. vinckei* isolate *PvCY*, was highly virulent and reached a parasitaemia of
154 $89.4\% \pm 1.4$ (standard error of mean; SEM) on day 6 post inoculation of 1×10^6
155 blood stage parasites intravenously, causing host mortality on that day. Both strains
156 of *P. v. brucechwatti*, *PvbDA* and *PvbDB*, were virulent and killed the host on day 7
157 or 8 post infection (peak parasitaemia of around 70%). The *P. v. lentum* parasites
158 *PvDS* and *PvDE*, were not lethal and were eventually cleared by the host immune
159 system, with *PvDS*'s clearance more prolonged than that of *PvDE* (parasitaemia
160 clearance rates; *PvDS* = 10.35 \%day^{-1} ; SE = 1.105; p-value of linear fit =0.0025;
161 *PvDE* = 16.46 \%day^{-1} ; SE = 3.873; p-value =0.023). The *P. v. petteri* isolates
162 *PvpCR* and *PvpBS* reached peak parasitaemia along similar timelines (6-7 dpi), but
163 *PvpCR* was virulent (peak parasitaemia = $60.35 \% \pm 2.38$ on day 6) and could
164 sometimes kill the host while *PvpBS* maintained a mild infection.

165

166 Of the three isolates of *P. vinckei baforti*, *PvsEL* and *PvsEE* were similar in their
167 growth profiles and their perceived effect on the host, while in contrast, *PvsEH* was
168 highly virulent, causing host mortality at day 5, the earliest among all *P. vinckei*
169 parasites.

170

171 RBC densities reduced during the course of infection proportionally to the rise in
172 parasitaemia in all the *P. vinckei* infection profiles studied. There were differences,
173 however, in the patterns of host weight loss. Mild infections by *P. v. lentum* isolates

174 (maximum weight loss in *Pv*DE = 0.43 mg \pm 0.41 and *Pv*DS = 1.77 mg \pm 0.38), *P. v.*
175 *petteri* BS (0.58 mg \pm 0.22) and *P. v. baforti* EE (1.66 mg \pm 0.31, 0.09 mg \pm 0.56) did
176 not cause any significant weight loss in mice, whereas the virulent strains, *P. v.*
177 *petteri* CR (4.04 mg \pm 0.18), *P. v. brucechwatti* isolates (*pvb*DA = 3.5 mg \pm 0.39 and
178 *pvb*DB = 2.05 mg \pm 1.68) caused around a 20% decrease in weight. Virulent strains
179 *Pv*CY (1.74 mg \pm 0.15) and *Pvs*EH (0.52 mg \pm 0.13) did not cause any significant
180 weight loss during their infection before host death occurred.

181

182 ***Plasmodium vinckei* reference genome assembly and annotation**

183 High-quality reference genomes for five *P. vinckei* isolates, one from each
184 subspecies; *P. v. vinckei* CY (*Pv*CY), *P. v. brucechwatti* DA (*Pvb*DA), *P. v. lentum*
185 DE (*Pv*DE), *P. v. petteri* CR (*Pvp*CR) and *P. v. baforti* EL (*Pvs*EL) were assembled
186 from single-molecule real-time (SMRT) sequencing. PacBio long reads of 10-20
187 kilobases (kb) and with a high median coverage of >155X across the genome
188 (Additional File 1) enabled *de novo* assembly of each of the 14 chromosomes as
189 single unitigs (high confidence contig) (see Table 1). PacBio assembly base call
190 errors were corrected using high-quality 350bp and 550bp insert PCRfree Illumina
191 reads. A small number of gaps remain in the assemblies, but these are mainly
192 confined to the apicoplast genomes and to the *Pvs*EL and *Pv*DE genomes that were
193 assembled from 10kB-long PacBio reads instead of 20kB. The *Pvp*CR and *Pv*CY
194 assemblies, with each chromosome in one piece, are a significant improvement over
195 their existing fragmented genome assemblies (available through PlasmoDB v.30).

196

197 *Plasmodium vinckei* genome sizes range from 19.2 to 19.5 Mb except for *Pv*CY
198 which has a smaller genome size of 18.3 Mb, similar to that of *P. berghei* (both

199 isolates are from the same Katanga region). While we were not able to resolve the
200 telomeric repeats at the ends of some of the chromosomes, all the resolved
201 telomeric repeats had the RMP-specific sub-telomeric repeat sequences
202 CCCTA(G)AA. The mitochondrial and apicoplast genomes were ~6Kb and ~30 kb
203 long respectively, except for the apicoplast genomes of *PvpCR* and *PvsEL* for which
204 we were able to resolve only partial assemblies due to low read coverage (see
205 Additional File 4).

206

207 Gene models were predicted by combining multiple lines of evidence to improve the
208 quality of those predictions. These include publicly available *P. chabaudi* gene
209 models, *de novo* predicted gene models and transcript models from strand-specific
210 RNA-seq data of different blood life cycle stages. Consensus gene models were then
211 manually corrected through comparative genomics and visualization of mapped
212 RNAseq reads. As a result, we annotated 5,073 to 5,319 protein-coding genes, 57-
213 67 tRNA genes and 40-48 rRNA genes in each *P. vinckei* genome. Functional and
214 orthology analyses with the predicted *P. vinckei* proteins showed that the core
215 genome content in *P. vinckei* parasites is highly conserved among the species and
216 are comparable to other rodent and primate malaria species.

217

218 ***Plasmodium vinckei* genome assemblies reveal novel structural variations**

219 Comparative analysis of *P. vinckei* and other RMP genomes shows that *P. vinckei*
220 genomes exhibit the same high level of synteny seen within RMP genomes, but with
221 a number of chromosomal rearrangements. These events can be identified by
222 breaks in synteny (synteny breakpoints- SBPs) observed upon aligning and
223 comparing genome sequences.

224

225 We aligned *P. vinckei* and other RMP genomes to identify synteny blocks between
226 their chromosomes. Similar to previous findings in RMP genomes [26, 41] (Additional
227 file 12A), we observed large scale exchange of material between non-homologous
228 chromosomes, namely three reciprocal translocation events and one inversion
229 (Figure 2A, Additional File 5 and 12). A pan-*vinckei* reciprocal translocation of
230 ~0.6Mb (with 134 genes) and ~0.4 Mb (with 99 genes) long regions between
231 chromosomes VIII and X was observed between *P. vinckei* and *P. berghei* (whose
232 genome closely resembles that of the putative RMP ancestor [41]). Within the *P.*
233 *vinckei* subspecies, two reciprocal translocations separate *P. v. petteri* and *P. v.*
234 *baforti* from the other three subspecies. One pair of exchanges (~1 Mb and ~0.55
235 Mb) was observed between chromosomes V and XIII, and another smaller pair
236 (~150Kb and ~70Kb) between chromosomes V and VI. These events have left the
237 Chromosomes V of *PvCY-PvbDA-PvIDE* and *PvpCR-PvsEL* groups with only a
238 ~0.15 Mb region of synteny between them, consisting of 48 genes while the
239 remaining 304 genes have been rearranged with chromosome VI and XII.

240

241 There also exists a small, *PvCY*-specific inversion of a ~100 kb region in
242 chromosome XIV. All the synteny breakage points (SBPs) were verified manually
243 and were supported by PacBio read coverage ruling out the possibility of a
244 misassembly at the breakpoint junctions. The SBPs in chromosomes V and VI were
245 near rRNA units, loci previously described as hotspots for such rearrangement
246 events [42, 43].

247

248 **A pan-RMP phylogeny reveals high genotypic diversity within the *P. vinckei***
249 **clade**

250 In order to re-evaluate the evolutionary relationships among RMPs, we first inferred
251 a well-resolved species-level phylogeny that takes advantage of the manually
252 curated gene models in eight available high-quality RMP genomes representing all
253 RMPs. A maximum-likelihood phylogeny tree was inferred through partitioned
254 analysis using RAxML, of a concatenated protein alignment (2,281,420 amino acids
255 long) from 3,920 single-copy, conserved core genes in eleven taxa (eight RMPs, *P.*
256 *falciparum*, *P. knowlesi* and *P. vivax*; see Figure 2B and Additional File 6).

257

258 In order to assess the genetic diversity within RMP isolates, we sequenced
259 additional isolates for four *P. vinckei* subspecies (*PvbDB*, *PvIDS*, *PvpBS*, *PvsEH* and
260 *PvsEE*), *P. yoelii yoelii* (*Pyy33X*, *PyyCN* and *PyyAR*), *P. yoelii nigeriensis* (*PynD*), *P.*
261 *yoelii killicki* (*PykDG*), *P. yoelii subsp.* (*PysEL*) and *P. chabaudi subsp.* (*PcsEF*)
262 (Additional File 1). This, along with existing sequencing data for 13 RMP isolates
263 (from [26, 44]), were used to infer an isolate-level, pan-RMP maximum likelihood
264 phylogeny based on 1,010,956 high-quality SNPs in non-subtelomeric genes that
265 were called by mapping all reads onto the *PvVCY* reference genome (Figure 2C and
266 Additional File 7). Both phylogenies were well-resolved with robust 100% bootstrap
267 support obtained for the amino-acid based phylogeny and 78% or higher bootstrap
268 support for the SNPs-based phylogeny (majority-rule consensus tree criterion was
269 satisfied at 50 bootstraps for both the phylogenies).

270

271 Both protein alignment-based and SNP-based phylogenies show significant
272 divergence among the *P. vinckei* subspecies compared to the other RMPs. All *P.*

273 *vinckei* subspecies have begun to diverge from their common ancestor well before
274 sub-speciation events within *P. yoelii* and *P. chabaudi*.

275

276 A total of 521,934 polymorphic positions were found within the *P. vinckei* core coding
277 regions consisting of 4,644 non-subtelomeric genes across *P. vinckei* isolates. The
278 Katangan isolate, *P. v. vinckei*, has undergone significant divergence from the
279 common *vinckei* ancestor and is the most diverged of any RMP subspecies
280 sequenced to date. Number of SNPs ranged from 292,240 to 318,344 in pair-wise
281 comparisons of isolates with *PvvcY*, with 4,237 to 4,263 genes (out of the 4,644
282 core genes) having at least 5 SNPs. *Plasmodium v. brucechwatti* has also diverged
283 significantly, while the divergence of *P. v. lentum* is comparable to that of *P. y.*
284 *nigeriensis*, *P. y. kilicki* and *P. c. subsp.* from their respective putative ancestors.
285 Genetic diversity within *P. v. petteri* and *P. v. baforti* isolates are similar to that
286 observed within *P. yoelii* and *P. chabaudi* isolates while *P. v. lentum* and *P. v.*
287 *brucechwatti* isolates have exceptionally high and low divergences respectively.
288 Number of SNPs in pair-wise comparisons between the closest subspecies, *P. v.*
289 *petteri* and *P. v. baforti*, ranged from 53,554 (*P. v. baforti* EE) to 69,454 (*P. v. baforti*
290 EL) with 2,358 genes having at least 5 SNPs.

291

292 Our robust phylogeny based on a comprehensive set of genome-wide sequence
293 variations confirms previous estimates of RMP evolution based on isoenzyme
294 variation [5] and gene sequences of multiple housekeeping loci [6, 7], except for the
295 placement of *P. y. nigeriensis* D which we show to be diverged earlier than *P. y.*
296 *kilicki* DG (supported by a bootstrap value of 100).

297

298 **Molecular evolution within *P. vinckei* isolates**

299 Using SNP data (Additional file 7), we then assessed the differences in selection
300 pressure on the geographically diverse *P. vinckei* isolates by calculating the gene-
301 wise Ka/Ks ratio as a measure of enrichment of non-synonymous mutations in a
302 gene (signifying positive selection). We first compared the Katangan isolate (*PvvcY*)
303 from the highland forests in the DRC with the non-Katangan isolates from the
304 lowland forests elsewhere.

305

306 We made pairwise comparisons of the four non-Katangan *P. vinckei* subspecies with
307 *P. v. vinckei* which revealed several genes under significant positive selection
308 (Figure 3C). Notably, we identified three genes involved in mosquito transmission,
309 namely, a gamete-release protein (GAMER), a secreted ookinete protein (PIMMS43,
310 previously known as PSOP25) and a thrombospondin-related anonymous protein
311 (TRAP), featuring in all Katangan/non-Katangan subspecies comparisons.

312

313 GAMER (PVVCY_1202630 being the representative ortholog in *P. v. vinckei*;
314 PBANKA_1225400 in *P. berghei*) had high Ka/Ks values in all comparisons (except
315 for *P. v. vinckei*-*P. v. brucechwatti*) and is essential for gamete egress [45].
316 PIMMS43 (PVVCY_1102000; PBANKA_1119200) and TRAP (PVVCY_1305250;
317 PBANKA_1349800) showed high Ka/Ks values in all comparisons and are essential
318 for ookinete evasion from mosquito immune system [46] and sporozoite infectivity of
319 mosquito salivary glands and host hepatocytes [47] respectively.

320

321 Several exported proteins and surface antigens were also identified to have
322 undergone positive selection. PVVCY_0100120 (PCHAS_0100651 being the gene

323 ortholog in *P. chabaudi*) has a circumsporozoite-related antigen PFAM domain
324 (PF06589) and is a conserved protein found in all RMPs except *P. berghei*.
325 PVVCY_1200100 (PBANKA_1002600) is a merozoite surface antigen, p41 [48] that
326 is secreted following invasion [49].

327

328 To assess presence of geographic location-specific selection pressures among the
329 lowland forest isolates, *P. v. brucechwatti*, *P. v. lentum* and *P. v. baforti* were
330 compared with *P. v. petteri* CR from the CAR. To see if similar selection pressures
331 have acted on other RMP species, we also analysed the *P. yoelii* and *P. chabaudi*
332 isolates from these regions that we had sequenced in this study.

333

334 Several exported and rhoptry-associated proteins were identified as been under
335 positive selection in each comparison but in contrast to comparisons with *P. v.*
336 *vinckei*, there was no overlap of positively selected genes among the non-Katangan
337 isolates. However, we identified a conserved rodent malaria protein of unknown
338 function (PVVCY_0501990; PBANKA_051950) that seems to be under significant
339 positive selection with high Ka/Ks values (ranging from 2.14 to 4.39) in all *P. vinckei*
340 comparisons except *P. v. petteri* - *P. v. baforti*. The *P. yoelii* ortholog of this protein
341 was also positively selected among *P. y. yoelii*, *P. y. nigeriensis* and *P. y. killicki* but
342 was not under selection within the *P. y. yoelii* isolates, signifying region-specific
343 selection pressures.

344

345 A 28kDa ookinete surface protein (P28; PVVCY_0501540; PBANKA_0514900)
346 seem to be under positive selection in the Nigerian *P. v. brucechwatti* as it features
347 in both *P. v. vinckei* - *P. v. brucechwatti* and *P. v. brucechwatti* - *P. v. petteri*

348 comparisons. The protein is also seen positively selected among corresponding
349 Nigerian and Central African Republic *P. yoelii* isolates (*P. y. nigeriensis* – *P. y.*
350 *yoelii*). A protein phosphatase (PPM8; PVVCY_0903370; PBANKA_0913400) has
351 also undergone positive selection in all three RMP species between CAR and Congo
352 isolates (*P. c. chabaudi*- *P. c. adami* comparison from [26]).

353

354 **Evolutionary patterns within the RMP multigene families**

355 We were able to accurately annotate members of the ten RMP multigene families in
356 the *P. vinckei* genomes owing to the well-resolved sub-telomeric regions in the
357 Pacbio assemblies and manually curated gene models (see Table 1 and Additional
358 file 8). *P. v. vinckei*, similar to its sympatric species, *P. berghei*, had a lower
359 multigene family repertoire with copy numbers strikingly less than other *P. vinckei*
360 subspecies (exceptions were the *pir*, *etramp* and lysophospholipase families).
361 Multigene family sizes in the four non-Katangan *P. vinckei* subspecies were similar
362 to *P. chabaudi* except for expansion in the *ema1* and *fam-c* multigene families
363 (Figure 3A).

364

365 Next, we inferred maximum likelihood-based phylogenies for the ten multigene
366 families, in order to identify structural differences amongst their members and to
367 determine family evolutionary patterns across RMP species and *P. vinckei*
368 subspecies (Figure 3B, Additional file 3 and 4). Overall, we identified robust clades
369 (with bootstrap value >70) that fell into the following categories, i) pan-RMP, with
370 orthologous genes from the four RMP species (dark grey), ii) *berghei* group, with
371 genes from *P. berghei* and *P. yoelii* alone, iii) *vinckei* group, with genes from *P.*
372 *chabaudi* and any or all *P. vinckei* subspecies, iv) *P. vinckei*, with genes only from *P.*

373 *vinckei* subspecies and v) non-Katangan, with genes from all *P. vinckei* subspecies
374 except *P. v. vinckei*.

375

376 In general, a high level of orthology was observed between *P. chabaudi* and *P.*
377 *vinckei* genes forming several *vinckei* group clades (marked in orange in Figure 3) in
378 contrast to more species-specific clades of paralogous genes being formed in *P.*
379 *berghei* and *P. yoelii*. Thus, family expansions in *P. chabaudi* and *P. vinckei* seem to
380 have occurred in the common *vinckei* group ancestor prior to speciation.

381 We rebuilt the phylogenetic trees for *pir*, *fam-a* and *fam-b* families in order to see if
382 the previously defined clades [25, 26] were also maintained in *P. vinckei*. Overall, we
383 were able to reproduce the tree structures for the three families using the ML method
384 with *P. vinckei* gene family members now added to them.

385

386 For *pirs*, we obtained four long-form and eight short-form clades as in [26] (Additional
387 file 9, tree 10) albeit with lower bootstrap support, possibly due to our overly stringent
388 automated trimming of the sequence alignment (see Methods). With a few
389 exceptions, *P. vinckei pir* genes majorly populated two clades - L1 and S7 and a
390 subclade S1g. These clades, previously shown to be *P. chabaudi*-dominant, hold
391 equal or near equal proportions of *P. vinckei pirs* too. The only other *P. chabaudi*-
392 dominant clade, L4, remains as a completely *P. chabaudi*-specific gene expansion.

393 No *P. vinckei* species- or subspecies-specific clades are evident except for two
394 subclades that could be inferred as *PvCY*-specific expansions within L1 and S7
395 (marked i and ii in Additional file 9, tree 10). Speciation of *P. vinckei* subspecies from
396 their common ancestor seems to have been accompanied by gene gain in L1 and S7
397 clades and gene loss in S1g subclade. There is an almost linear increase of around

398 20 genes in *PvvCY*, *PvbDA* and *PvIDE* in clade L1 pirs and a near doubling of clade
399 S7 pirs in *PvpCR*.

400

401 The *fam-a* and *fam-b* phylogenies (Additional file 9, tree 3 and 4 respectively) show
402 that previously identified ancestral lineages [25] are maintained in *P. vinckei* too. The
403 addition of *P. vinckei* genes resolved the ancestral clade of internal *fam-a* genes in
404 chromosome 13 further into several well-supported *vinckei* group clades and a
405 *berghei* group clade (marked as A in Additional file 9, tree 3). The 19 other *fam-a*
406 clades and five *fam-b* clades consisting of positionally conserved orthologous genes
407 are also conserved in *P. vinckei* (pan-RMP clades marked with * in Additional file 9,
408 tree 3 and 4). The *fam-a* family has expanded in the non-Katangan *P. vinckei*
409 subspecies through independent events of gene duplication in their common
410 ancestor giving rise to several non-Katangan clades (marked as B in Additional file 9,
411 tree 3). There is only a moderate *P. vinckei*-specific expansion in *fam-b* giving rise to
412 three clades (marked as A in Additional file 9, tree 4) that includes *PvvCY* genes too,
413 pointing to gene duplications in the *P. vinckei* common ancestor. In both the
414 phylogenies, species and subspecies-specific gene duplication events within the
415 *vinckei* group are rare but do occur (marked as i-iv in Additional file 9, tree 3 and 4).

416

417 The *fam-d* multigene family is present as a single ancestral copy in *P. berghei*
418 internally on chromosome IX but is expanded into a gene cluster in the same loci in
419 *P. yoelii* (5 genes) and *P. chabaudi* (21 genes). Similar expansions have occurred in
420 *P. vinckei* subspecies and phylogenetic analysis shows the presence of six robust
421 clades within this family (Additional file 9, tree 6). Clade I is clearly the ancestral
422 clade from which all other *fam-d* genes have been derived as it consists of the single

423 *P. berghei* gene and its orthologs in other RMPs, positionally conserved to be the
424 outermost gene of the *fam-d* cluster in each RMP.

425

426 While the *fam-d* family in *P. yoelii* is completely a product of paralogous expansion
427 within Clade I, the *fam-d* families in the *vinckei* group seem to have expanded *via*
428 five ancestral lineages forming clades II-VI. A subset of orthologs in Clade II (marked
429 with * in Additional file 9, tree 6) are positionally conserved among *vinckei* group
430 parasites, located immediately after the *fam-d* ancestral copy and could therefore
431 represent the Clade II ancestral gene in the *vinckei* group common ancestor. *Pv*CY
432 has a smaller *fam-d* repertoire of 6 genes derived from only three of the five *vinckei*
433 group lineages (Clade II, IV and VI), apart from the conserved ancestral copy.

434

435 ML-based trees for haloacid dehalogenase-like hydrolase (*hdh*), putative reticulocyte
436 binding proteins (*p235*) and lysophospholipases (*lp1*) have generally well-resolved
437 topologies with robust bootstrap support for their nodes and some clades contain
438 syntenic orthologous genes (clades marked with * in Additional file 9, trees 7, 8 and
439 9) to member genes in *P. falciparum*, for example, *PfHAD2*, *PfHAD3*, *PfHAD4* and
440 *PfRH6*. Poor bootstrap support was obtained for the *etramp* tree (Additional file 9,
441 tree 2), however clades were identified for some members including *uis3*, *uis4* and
442 *etramp10.2*.

443

444 In order to assess the general level of expression of multi-gene family members in
445 blood stage parasites, we superimposed blood-stage RNAseq data onto the
446 phylogenetic trees. Life stage specific expression of multigene family members in
447 five RMPs – *P. berghei* (rings, trophozoites, schizonts and gametocytes) [26], *P.*

448 *chabaudi* and *P. v. vinckei* (rings, trophozoites and schizonts) [50], *P. v. petteri* and
449 *P. v. lentum* (rings, trophozoites and gametocytes) and mixed blood stage
450 expression levels in *P. yoelii* [44], *P. v. brucechwatti* and *P. v. baforti* were assessed
451 (Additional File 10).

452

453 The level of gene transcription was designated low for genes with normalized FPKM
454 (Fragments Per Kilobase of transcript per Million mapped reads) less than 36,
455 medium if between 36 and 256 and high for genes with FPKM above 256. Both the
456 levels and life stage specificity of gene expression within the various clades were
457 generally conserved across the RMPs signifying that orthologs in structurally distinct
458 clades might have conserved functions across the different RMPs. In general, the
459 proportion of transcribed genes in all multigene families in *P. vinckei* was similar to
460 that observed in *P. chabaudi* and slightly higher than *P. berghei* and *P. yoelii*
461 (excluding the families with only one or two *P. berghei* or *P. yoelii* members).

462

463 **The erythrocyte membrane antigen 1 and *fam-c* sub-telomeric multigene**
464 **families are expanded in non-Katangan *P. vinckei* parasites.**

465 The erythrocyte membrane antigen 1 (EMA1) was first identified and described in *P.*
466 *chabaudi* and is associated with the host RBC membrane [51]. These genes encode
467 for a ~800 aa long protein and consist of two exons; a first short exon carrying a
468 signal peptide followed by a longer exon carrying a PcEMA1 protein family domain
469 (Pfam ID- PF07418). The gene encoding EMA1 is present only as a single copy in *P.*
470 *yoelii* or as two copies in *P. berghei* but has expanded to 14 genes in *P. chabaudi*.
471 We see similar gene expansions of 15 to 21 members in the four non-Katangan *P.*
472 *vinckei* parasites (*PvbDA*, *PvIDE*, *PvpCR* and *PvsEL*; Figure 3A and Additional file

473 3). However, almost half of these genes are pseudogenes with a conserved SNP
474 (C>A) at base position 14 that introduces a TAA stop codon (S5X) within the signal
475 peptide region, followed by a few more stop codons in the rest of the gene (see
476 Additional File 12B). Apart from one or two cases, the S5X mutation is found in all
477 pseudogenes belonging to the *ema1* family and is *vinckei*-specific (it is not present in
478 the single *P. chabaudi* pseudogene).

479

480 A ML-based phylogeny inferred for the 99 *ema1* genes was in general well-resolved
481 with robust branch support for most nodes (see Figure 3B). Four distinct *vinckei*
482 group-specific clades (Clade I to IV), two *vinckei*-specific clades (Clade IV and V)
483 and a non-Katangan *P. vinckei* - specific clade (VI) with good basal support
484 (bootstrap value of 75-100) were identified. Clade I-IV each consist of *ema1* genes
485 positionally conserved across *P. chabaudi* and all five *P. vinckei* subspecies (in
486 chromosomes I, VII, IX and X respectively) and are actively transcribed during blood
487 stages.

488

489 Of the two *P. berghei* *ema1* genes, one forms a distal clade with the single *P. yoelii*
490 gene while the other is paraphyletic within Clade IV, pointing to presence of two
491 *ema1* loci in the common RMP ancestor, one of which was possibly lost during
492 speciation of *P. yoelii*. All seven *PvCY* *ema1* genes are found within clades I to V
493 with gene duplication events in Clade III and V.

494

495 Family expansion in *P. chabaudi* is mainly driven by gene duplication giving rise to *P.*
496 *chabaudi*-specific clades. In contrast, family expansion within non-Katangan *P.*
497 *vinckei* parasites is mainly driven by expansion of pseudogenized *ema1* genes (41

498 genes). Except for some *P. v. brucechwatti*-specific gene expansions, the
499 pseudogenes do not form subspecies-specific clades suggesting that the expansion
500 must have occurred in their non-Katangan *P. vinckei* common ancestor.

501

502 Gene expression data shows that the members of the *P. vinckei*-specific Clade IV
503 are heavily transcribed during blood stages but most *ema1* pseudogenes that share
504 ancestral lineage with Clade IV are very weakly transcribed. Taken together, a core
505 repertoire of conserved *ema1* genes arising from 4-5 independent ancestral lineages
506 are actively transcribed during blood stages of *P. vinckei* and *P. chabaudi*. The *ema1*
507 multigene family expansion in *P. vinckei* is largely due to duplications of *ema1*
508 pseudogenes, all carrying a S5X mutation and lacking transcription.

509

510 The *fam-c* proteins are exported proteins characterized by *pyst-c1* and *pyst-c2*
511 domains, first identified in *P. yoelii* [42]. There is a considerable expansion of this
512 family in the non-Katangan *P. vinckei* strains resulting in 59 to 65 members, twice
513 that of *PwCY* and other RMPs. The *fam-c* genes are exclusively found in the sub
514 telomeric regions and are composed of two exons and an intron, of which the first
515 exon is uniformly 80 bps long (with a few exceptions). *fam-c* proteins are
516 approximately 100-200 amino acids long, and more than one third of the proteins in
517 *P. vinckei* contain a transmembrane domain (75.5%) and a signal peptide (88.9%)
518 but most of them lack a PEXEL-motif (motif was detected in only 4% of the genes
519 compared to 24% in other RMPs).

520

521 An ML-based tree of all *fam-c* genes in the eight RMP species shows the presence
522 of four distinctly distal clades (marked as A in Figure 3B) with robust basal support

523 (96-100). Two of them are pan-RMP and two are *vinckei* group-specific, each
524 consisting of *fam-c* genes positionally conserved across the member subspecies
525 (taking into account the genome rearrangement between chromosome V and VI
526 within the *vinckei* clade). Most members of these clades show medium to high gene
527 expression during asexual blood stages.

528

529 The remainder of the tree's topology does not have good branch support (<70) with
530 the exception of some terminal nodes, but it does demonstrate the significant
531 expansion of this gene family within non-Katangan *P. vinckei* parasites (clades
532 shaded in blue).

533

534 There is evidence of significant species- and subspecies-specific expansions with
535 striking examples in *P. yoelii*, *P. chabaudi* and in *P. v. brucechwatti* (marked i, ii and
536 iii in Figure 3B respectively), though they do not form well-supported clades. Most
537 *fam-c* genes in *P. yoelii* seem to have originated from such independent *P. yoelii* -
538 specific expansion events. *P. chabaudi* and *P. v. vinckei* *fam-c* genes are found
539 more widely dispersed throughout the tree suggesting divergence of this family in the
540 *vinckei* group common ancestor. On the other hand, subspecies-wise distinctions
541 among the non-Katangan *P. vinckei* *fam-c* genes are less resolved as they form both
542 paralogous and orthologous groups between the four subspecies with several
543 ortholog pairs strongly supported by bootstrap values.

544

545 Thus, *fam-c* gene family expansion in the non-Katangan *P. vinckei* subspecies
546 seems to have been driven by both gene duplications in their common ancestor and
547 subspecies-specific gene family expansions subsequent to subspeciation. Around

548 half of the *fam-c* genes have detectable transcripts in asexual or sexual blood
549 stages. Most of the transcribed genes have medium ($36 < \text{FPKM} < 256$) or high-level
550 expression ($\text{FPKM} > 256$) and blood-stage specific expression data for *P. chabaudi*
551 and *P. v. vinckei* show peak transcription among the asexual blood stages at ring
552 and schizont stages.

553

554 **Genetic crossing can be performed between *P. vinckei* isolates**

555 The availability of several isolates within each *P. vinckei* subspecies with varying
556 growth rates and wide genetic diversity makes them well-suited for genetic studies.
557 Therefore, we attempted genetic crossing of the two *P. vinckei baforti* isolates,
558 *PvsEH* and *PvsEL*, that displayed differences in their growth rates. Optimal
559 transmission temperature and vector stages were initially characterized for *P. v.*
560 *baforti* EE, EH and EL. Each isolate was inoculated into three CBA mice and on day
561 3 post infection, around 100 female *A. stephensi* mosquitoes were allowed to
562 engorge on each mouse at different temperatures - 21°C, 23°C and 26°C. All three
563 *P. v. baforti* isolates were able establish infections in mosquitoes at 23°C and 26°C,
564 producing at least 50 mature oocysts on day 15 post-feed, but failed to transmit at
565 21°C (Figure 1A (a) and Additional file 6). Four to five oocysts of 12.5-17.5 µm
566 diameter were observed at day 8 post-feed in the mosquito midgut and around a
567 hundred mature oocysts of 50 µm diameter could be observed at day 15 post-feed.
568 Some of these mature oocysts had progressed into sporozoites but only a very few
569 appeared upon disruption of the salivary glands.

570

571 To perform a genetic cross between *PvsEH* and *PvsEL*, a mixed inoculum containing
572 equal proportions of *PvsEH* and *PvsEL* parasites was injected into CBA mice and a

573 mosquito feed was performed on both day 3 and day 4 post-infection to increase the
574 chances of a successful transmission (Additional 7 B). For each feed, around 160
575 female *A. stephensi* mosquitoes were allowed to take a blood meal from two
576 anaesthetized mice at 24°C for 40 minutes without interruption.

577

578 Upon inspection of mosquito midguts for the presence of oocysts on day 9 post-feed,
579 100% infection was observed (all midguts inspected contained oocysts) for both day
580 3 and day 4 feeds. Around 25-100 oocysts were found per midgut in day 3 fed
581 mosquitoes and 5-40 oocysts per midgut in day 4 fed mosquitoes. On day 12 post-
582 feed, mature oocysts and also a high number of sporozoites were found in the
583 midguts, but upon disrupting the salivary glands on day 20 post-feed, only a few
584 sporozoites were found in the suspension.

585

586 Sporozoites from day 3 and 4 fed mosquitoes were injected into ICR mice (D3 and
587 D4 respectively) and five days later, both mice became positive for blood stage
588 parasites. In order to confirm that a genetic cross has taken place, four clones were
589 obtained from D4 by limiting dilution to screen for presence of both *PvsEH* and
590 *PvsEL* alleles within the chromosomes. Based on the SNPs identified between
591 *PvsEH* and *PvsEL*, we amplified 600 to 1,000 bp regions from polymorphic genes on
592 both ends of the 14 chromosomes that contained isolate-specific SNPs and
593 performed Sanger sequencing of the amplicons (primer sequences in Additional file
594 6).

595

596 Both *PvsEL*-specific (11) and *PvsEH*-specific (17) markers were found in the 28
597 markers sequenced (one marker, PVSEL_0600390, could not be amplified). Also,

598 five chromosomes clearly showed evidence of chromosomal cross-over since they
599 contained markers from both isolates (see Figure 4A), thus confirming a successful
600 *P. vinckei* genetic cross. However, all four clones had the same pattern of
601 recombination which suggests that the diversity of recombinants in the cross-
602 progeny was low and a single recombinant parasite might have undergone
603 significant clonal expansion.

604

605 ***P. vinckei* parasites are amenable to genetic manipulation**

606 We asked if *P. vinckei* parasites can be genetically modified by applying existing
607 transfection and genetic modification techniques routinely used in other RMPs.
608 *Plasmodium v. vinckei* CY was chosen to test this because the isolate naturally
609 established a synchronous infection in mice and reaches a high parasitaemia, which
610 results in an abundance of schizonts for transfection. We aimed to produce a *Pv*CY
611 line that constitutively expresses GFP_{Luc} (green fluorescent protein- firefly
612 luciferase) fusion protein, similar to those produced in *P. berghei* and *P. yoelii* [52,
613 53]. A recombination plasmid, *pPvCY-Δp230p-gfpLuc*, was constructed to target
614 and replace the dispensable wildtype P230p locus in *P. v. vinckei* CY
615 (PVVCY_0300700) with a gene cassette encoding for GFP_{Luc} and a *hdhfr*
616 selectable marker cassette (Figure 4B).

617

618 Transfection of purified *Pv*CY schizonts with 20 μg of linearized *pPvCY-Δp230p-*
619 *gfpLuc* plasmid by electroporation, followed by marker selection using
620 pyrimethamine yielded pyrimethamine-resistant transfectant parasites (*Pv*GFP-
621 *Luc_{con}*) on day 6 after drug treatment. Stable transfectants were cloned by limiting
622 dilution and plasmid integration in these clones was confirmed by PCR. Constitutive

623 expression of GFP_{Luc} in PvGFP-Luc_{con} asexual and sexual blood stage parasites
624 was confirmed by fluorescence live cell imaging (Figure 4C). GFP_{Luc} expression in
625 PvGFP-Luc_{con} oocysts was confirmed by fluorescence imaging of mosquito midguts
626 7 days after blood meal.

627

628 **Discussion**

629 Of the four RMP species that have been adapted to laboratory mice, *P. berghei*, *P.*
630 *yoelii* and *P. chabaudi* have been extensively used to investigate malaria parasite
631 biology. Adopting these RMPs as tractable experimental models has been facilitated
632 by continuous efforts in characterizing their phenotypes, sequencing their genomes
633 and establishing protocols for parasite maintenance, genetic crossing and genetic
634 modification. Here, we extend these efforts to *Plasmodium vinckei*.

635

636 We have systematically studied ten *P. vinckei* isolates and produced a
637 comprehensive resource of their reference genomes, transcriptomes, genotypes and
638 phenotypes to help establish *P. vinckei* as a useful additional experimental model for
639 malaria.

640

641 Enzyme variation and molecular phylogeny studies indicate that the five subspecies
642 of *P. vinckei* have diverged significantly from each probably due to the geographical
643 isolation of these parasites in different locations around the African Congo basin.
644 This diversity calls for a reference genome for each subspecies in order to capture
645 large-scale changes in their genomes such as chromosomal structural variations and
646 gene copy number variations that might have played a role in their speciation. To
647 accurately capture these events, we used a combination of Pacbio and Illumina

648 sequencing that allowed us to produce an end-to-end assembly of *P. vinckei*
649 chromosomes. This, coupled with manual curation of the predicted gene models, led
650 to the creation of five high-quality reference genomes for *P. vinckei* that are a
651 significant improvement to the existing fragmented genomes available for *P. v.*
652 *vinckei* and *P. v. petteri*.

653

654 Comparative synteny analysis between *P. vinckei* and other RMP genomes reveals
655 structural variations at both the species and the subspecies levels. Assuming that
656 the observed variations have occurred only once, a putative pathway of genome
657 rearrangements during RMP evolution can be inferred. No rearrangements have
658 occurred during *P. berghei* and *P. yoelii* speciation and their genomes are likely to be
659 identical to the RMP ancestor [41]. A reciprocal translocation between chromosomes
660 VIII and X has accompanied the speciation of *P. vinckei*, and this is mutually
661 exclusive from the reciprocal translocation between chromosome VII and IX that has
662 occurred during *P. chabaudi* speciation. Following this, there has been a small
663 inversion in chromosome X during the subspeciation of *P. v. vinckei* and
664 translocations between chromosomes V, VI and XIII during the subspeciation of *P. v.*
665 *petteri* (which are then carried over to *P. v. baforti*).

666

667 We generated additional sequencing data for several *P. vinckei* isolates and made
668 available at least two genotypes per *P. vinckei* subspecies (except for *P. v. vinckei*
669 for which only one isolate is available) so as to facilitate future studies that might
670 employ *P. vinckei* parasites to study phenotype-genotype relationships. Similarly, we
671 also supplemented the existing genotype information for other RMPs by sequencing
672 several isolates from additional subspecies of *P. chabaudi* and *P. yoelii*. Our data

673 thus comprises of genotypes from sympatric species from each region of isolation
674 allowing us to re-evaluate the genotypic diversity and evolution among RMP isolates.

675

676 A genome-wide SNP-based phylogeny shows that the divergences between different
677 subspecies are proportional to the level of isolation of the habitat for all RMP
678 species. *Plasmodium vinckei*, *P. yoelii* and *P. chabaudi* isolates from sites in
679 Cameroon have very similar genotypes to their counterparts in the Central African
680 Republic denoting similar evolutionary pressures and perhaps the presence of gene
681 flow across these regions, while isolates from Brazzaville (Congo) are more
682 diverged probably due to the different environmental conditions in these locations
683 [40].

684

685 Subspecies from West Nigeria and the DRC are highly diverged compared to
686 subspecies from the rest of Africa. The distinctiveness of *P. berghei* and *P. v.*
687 *vinckei*, both from the DRC is most likely due to climatic and host-vector differences
688 in the highland forests of Katanga. Highland forests are an altitude of 1000-7000 m
689 with mean temperature of 21C whereas the lowland forests lie at an altitude less
690 than 800m with a mean temperature of 25 C. Different host-vector systems are
691 prevalent in the lowland forests (*Grammomys poensis* (previously known as
692 *Thamnomys rutilans*) - specific mosquito species unknown) and the highland
693 Katangan forests (*Grammomys surdaster* -*Anopheles durenii millecampsii*). The
694 associated selection pressures seem to have mainly influenced their transmission,
695 as reflected by their lower optimal transmission temperatures and the high Ka/Ks
696 ratios observed for three proteins that play critical functions in this process. Recently,
697 several more rodent host and mosquito vector species have been identified in the

698 forests of Gabon [54] implying that a diverse set of host-vector systems could have
699 existed for RMPs. Thus, diversification of RMP species into several subspecies
700 within these isolated ecological niches might have been driven by evolutionary forces
701 resulting from the diverse host, vector and environmental conditions experienced at
702 each locale.

703

704 Malaria parasite genomes contain several highly polymorphic multigene families
705 located in the sub-telomeric chromosomal regions that encode a variety of exported
706 proteins involved in processes such as immune evasion, cytoadherence, nutrient
707 uptake and membrane synthesis. Multigene families are thought to have evolved
708 rapidly under the influence of immune and other evolutionary pressures resulting in
709 copy number variations and rampant sequence reshuffling that ultimately leads to
710 phenotypic plasticity in *Plasmodium*.

711

712 Previously, phylogenetic analyses of *pir*, *fam-a* and *fam-b* genes from three RMP
713 species have shown that structurally distinct genes exist within these families
714 forming robust clades with varied levels of orthology/paralogy. Identifying sub-
715 families that have structurally diversified within the multigene families can help to
716 better understand their functions and to this end, we constructed phylogenetic trees
717 for the ten multigene families with genes from all four RMP species. Due to the scale
718 of the analysis, we applied automated trimming to our alignments and limited our
719 tree inference method to maximum likelihood. While this resulted in poor bootstrap
720 values for some clades in the *pir*, *fam-a* and *fam-b* trees compared to previous
721 phylogenetic analyses [25, 26], our method was able to retrieve similar tree

722 topologies to those previously inferred and in general produced trees with good
723 nodal support for the rest of the multigene families.

724

725 Robust pan-RMP clades identified in our study represent ancestral lineages
726 consisting of structural orthologs that perform conserved functions across all RMPs
727 and will be useful for future work with these families. We show that certain ancestral
728 lineages can expand in a particular species or subspecies in response to selective
729 pressures resulting in distinct evolutionary histories for each family. For example, the
730 *pir* family expansion is mostly species-specific and driven by frequent gene
731 conversion after speciation, whereas the expansion of the *fam-a* gene repertoire
732 seems to have occurred initially in the RMP ancestor followed by species-specific
733 expansions.

734

735 Inclusion of *P. vinckei pirs* in the RMP *pir* family phylogeny show that *P. vinckei pirs*
736 do not form independent clades of their own and instead populate three *P. chabaudi*-
737 dominant clades. This suggests that some of the *pir* clades were established earlier
738 on when the classical *vinckei* and *berghei* group of parasites split from their common
739 RMP ancestor resulting in *vinckei* group-specific clades like L1, S7 and S1g.

740

741 Similarly, the addition of *P. vinckei* genes resolved the ancestral clade of internal
742 *fam-a* genes into several well-supported *vinckei* group clades and a *berghei* group
743 clade. We observe similarly high level of orthology between *P. chabaudi* and *P.*
744 *vinckei* genes in other multigene families forming several *vinckei* group clades in
745 contrast to more species-specific clades of paralogous genes in *P. berghei* and *P.*
746 *yoelii*. For example, within the *fam-d* family, five ancestral lineages can be identified

747 in the *vinckei* group as opposed to only one paralogous *P. yoelii*-specific expansion
748 within the *berghei* group. Taken together, it seems that family expansions in *P.*
749 *chabaudi* and *P. vinckei* have occurred in the common *vinckei* group ancestor prior
750 to speciation and that multigene families have evolved quite differently across the
751 *vinckei* and *berghei* groups of RMPs. These might be related to the striking
752 differences in the basic phenotypes of these two groups of parasites.

753

754 We also observed size expansions in the *ema1* and *fam-c* families within the non-
755 Katangan *P. vinckei* parasites, all being isolates from the lowlands around the Congo
756 Basin. *Ema1* family expansions seem to be specific to lowlands dwelling *vinckei*
757 group parasites as they are expanded in both non-Katangan *P. vinckei* and *P.*
758 *chabaudi*. However, unlike *P. chabaudi*, the duplicated gene members in non-
759 Katangan *P. vinckei* are all pseudogenized by a S5X mutation effectively rendering
760 the functional repertoire to be just 6-8 genes, similar to highlands dwelling Katangan
761 *P. v. vinckei*. Thus, it could be speculated that even under similar selective
762 pressures, *ema1* family expansions contribute to parasite fitness in *P. chabaudi* but
763 may not be required for the survival of sympatric *P. vinckei* parasites. The *P. vinckei*
764 *ema1* pseudogenes could still serve as silent donor genes that recombine into
765 functional variants to bring about antigenic variation [55]. In the case of the *fam-c*
766 gene family, the expansion is specific to non-Katangan *P. vinckei* subspecies since
767 *P. chabaudi*, *P. yoelii* and *P. v. vinckei* all have similar repertoire sizes. The
768 expansions seem to be driven by gene duplications initially in their non-Katangan
769 common ancestor and again after subspeciation.

770

771 The effect of the difference in habitats is even more pronounced in the Katangan
772 parasite, *P. v. vinckei*. It has a smaller genome and a compact multigene family
773 repertoire reminiscent of the only other Katangan isolate, *P. berghei* and its genetic
774 distance from other members of the *P. vinckei* clade is in the same order of
775 magnitude as that between separate species within the RMPs. The reduced
776 multigene family repertoire mainly consists of members belonging to pan-RMP or
777 *vinckei*-group specific ancestral lineages making it an ideal *vinckei* group parasite to
778 study the localization and function of variant proteins.

779

780 We tested whether *PvCY* was amenable to genetic manipulation using standard
781 transfection protocols already established for other RMPs. We were able to
782 successfully knock-in a GFP-luciferase fusion cassette to *PvCY* to produce a GFP-
783 Luc reporter line for *P. v. vinckei*, following a transfection protocol routinely used for
784 modifying *P. yoelii* in our lab [44, 56]. We were able to visualise GFP-positive
785 parasites during different blood stages and in oocysts thus confirming stable GFP-Luc
786 expression. We were unable to visualise other life stages (sporozoites and liver
787 stages) due to our failure to produce viable salivary gland sporozoites in this
788 parasite.

789

790 The transfection of *P. chabaudi* has been challenging due to its slow proliferation
791 rate and schizont sequestration resulting in low merozoite yield, thus necessitating
792 optimized transfection protocols. In contrast, *Plasmodium v. vinckei* reaches high
793 parasitaemia without being immediately lethal to the host (90% parasitaemia on day
794 6) and is highly synchronous yielding a large number of schizonts. A predominant
795 population of schizonts appear near midnight in *P. v. vinckei* infections, at which

796 point, they can be Percoll-purified from exsanguinated blood and transfected with
797 DNA.

798

799 *P. vinckei* and *P. chabaudi*, while being distinct species, share several
800 characteristics that are common among *vinckei* group RMPs, such as a predilection
801 for mature erythrocytes, synchronous infections and the sequestration of schizonts
802 from peripheral circulation [33, 37, 57-59]. Thus, *P. v. vinckei* can serve as an ideal
803 experimental model for functional studies targeting these aspects of parasite biology.

804

805 The availability of several RMP isolates with phenotypic differences aids their use in
806 study of parasite fitness and transmission success in mixed infections [60, 61] and
807 for the identification of genes involved in parasite virulence, strain-specific immunity,
808 drug resistance and host-cell preference using genetic crosses [44, 62-64]. With this
809 in mind, we studied the virulence of ten *P. vinckei* isolates to identify differences in
810 their growth rate and their effect on the host.

811

812 Some of these isolates have been previously characterized [40], but we
813 systematically profiled additional representative isolates for each subspecies (where
814 available) under comparative conditions in the same host strain. We identified pairs
815 of isolates with contrasting virulence phenotypes within two *P. vinckei* subspecies –
816 *P. v. petteri* (*PvpCR* and *PvpBS*) and *P. v. baforti* (*PvsEH* and *PvsEL* or *PvsEE*).
817 These isolate pairs would be ideal candidates for studies utilising genetic crossing to
818 identify genetic *loci* linked to virulence using Linkage Group Selection [44].

819

820 Since *P. vinckei* subspecies have significantly diverged from each other, isolates
821 within the same subspecies are more likely to recombine than isolates from different
822 subspecies. However, intra-specific hybrids between *P. v. petteri* and *P. v. baforti*
823 may also be possible (as demonstrated earlier in *P. yoelii* [65]) since these two
824 subspecies are closely related (see Figure 2C). However, difficulties in transmitting
825 *P. vinckei* parasites have been reported previously with either the gametocytes
826 failing to produce midgut infections or sporozoites failing to invade the salivary
827 glands or infections resulting in non-infective sporozoites [27, 30, 35]. Repeated
828 attempts to create a cross between two *P. vinckei baforti* isolates failed to produce
829 any detectable recombinants due to low frequency of mosquito transmission [35].
830 Here, we renewed these efforts with different *P. vinckei* isolates to see if we could
831 establish a *P. vinckei* genetic cross. Two attempts were made to create a *pvpCR* X
832 *pvpBS* cross and further two attempts were made to create a *pvsEL* X *pvsEH* cross.
833 However, in all attempts the sporozoites failed to optimally invade the salivary glands
834 and we managed to isolate only a few in the *P. v. subsp* cross, subsequently
835 obtaining a cross progeny in mice. While we were able to demonstrate a successful
836 genetic cross by showing the presence of alleles from both isolates in the cross
837 progeny, the recombinant diversity was quite low probably due to the transmission
838 bottleneck. We are currently further investigating the optimal conditions for
839 transmitting *P. vinckei*.

840

841 **Conclusions**

842 In this study, we have created a comprehensive resource for the rodent malaria
843 parasite *Plasmodium vinckei*, comprising of five high-quality reference genomes, and
844 blood stage-specific transcriptomes, genotypes and phenotypes for ten isolates. We

845 have employed state-of-the-art sequencing technologies to produce largely complete
846 genome assemblies and highly accurate gene models that were manually polished
847 based on strand-specific RNA sequencing data. The unfragmented nature of our
848 genome assemblies allowed us to characterize structural variations within *P. vinckei*
849 subspecies, which, to the best of our knowledge, is the first time that large-scale
850 genome re-arrangements have been found among subspecies of a *Plasmodium*
851 species.

852

853 The biological or phenotypic significance, if any, of such alterations are poorly
854 understood, but it seems likely that they may drive speciation through the promotion
855 of reproductive isolation of species or subspecies. Through our extensive
856 sequencing efforts, we have generated genotype data for seventeen RMP isolates
857 comprising of five *P. vinckei*, four *P. yoelii* and one *P. chabaudi* subspecies, thus
858 making at least one genotype available for all subspecies of the RMP that previously
859 lacked any sequencing data. We also systematically characterised the virulence
860 phenotypes of the ten *P. vinckei* isolates to capture the phenotypic diversity among
861 them. Combined, these efforts will greatly aid genetic linkage studies to resolve
862 genotype-phenotype relationships.

863

864 In order to understand the evolutionary relationships among the RMP isolates, we
865 have carried out a combination of analyses to describe the genotypic diversity
866 molecular evolution of these parasites. While our phylogenies more or less agree
867 with previous biochemical and molecular data-based studies, our reconstruction
868 based on sequence variations on a genome scale provides higher resolution to the
869 divergence estimates. Taking advantage of the high-quality RMP genomes produced

870 from our work and previous studies, we also undertook a comprehensive
871 phylogenetic analysis of multigene families across all RMP species and identify
872 various structurally diversified sub-families with distinct evolutionary histories. This
873 will enable future studies on the critical role of multigene families in parasite
874 adaptation, and to aid this, we have made searchable and interactive versions of the
875 phylogenies publicly available through the iTOL online tool [66].

876

877 While genome rearrangements have occurred during speciation and sub speciation
878 events, diversification of the multigene families seem to have occurred earlier when
879 the RMPs split into *vinckei* and *berghei* groups of parasites. Thus, structural, copy
880 number and nucleotide-level variations among the RMPs have occurred at various
881 points during the evolution of RMPs in response to a variety of evolutionary
882 pressures. The gene expression data from our study, covering specific blood stages
883 for some *P. vinckei* subspecies, show conserved expression of multigene family
884 members across RMPs. While not comprehensive, it complements existing RMP
885 transcriptomes and will aid functional studies in the *P. vinckei* model. Taken
886 together, our study provides a comprehensive view of the phenotypic and genotypic
887 diversity within RMPs and functional diversification of the multigene families in
888 response to selection pressures.

889

890 The synchronicity of *P. v. vinckei* infection and its unique ability to sustain high
891 parasitaemia without killing its host culminating in good schizont yields make this
892 parasite an attractive model for reverse genetics studies, especially those on
893 multigene families owing to its reduced repertoire. We have successfully
894 demonstrated genetic manipulation in *P. v. vinckei* but encountered difficulties in

895 producing large numbers of recombinant parasites through genetic crossing.
896 Attempts to transmit isolates from three different *P. vinckei* subspecies in *A.*
897 *stephensi* mosquitoes failed in our hands as sporozoites repeatedly failed to infect
898 the salivary glands. Careful optimisation of transmission parameters and serial
899 mosquito passages of the *P. vinckei* parasites might help in improving their
900 transmission efficiency and could aid genetic linkage studies with these parasites.

901

902

903

904 **Methods**

905 **Parasite lines and experiments using mice and mosquitos**

906 The parasite lines used in this study and their original isolate information are detailed
907 in Supplementary Table 1. Frozen parasite stabilates of cloned or uncloned lines
908 were revived and inoculated intravenously into ICR mice. Five *P. vinckei* isolates
909 (*Pvvcy*, *Pvbda*, *Pvbdb*, *PvIde* and *PvsEE*) and the *P. yoelii nigeriensis* isolate
910 (*PynD*) were uncloned stabilates and were cloned by limiting dilution to obtain clonal
911 parasite lines.

912

913 Laboratory animal experimentation was performed in strict accordance with the
914 Japanese Humane Treatment and Management of Animals Law (Law No. 105 dated
915 19 October 1973 modified on 2 June 2006), and the Regulation on Animal
916 Experimentation at Nagasaki University, Japan. The protocol was approved by the
917 Institutional Animal Research Committee of Nagasaki University (permit:
918 12072610052).

919

920 Six to eight weeks old female ICR or CBA mice were used in all the experiments.
921 The
922 mice were housed at 23°C and maintained on a diet of mouse feed and water. Mice
923 infected with malaria parasites were given 0.05% para-aminobenzoic acid (PABA)-
924 supplemented water to assist parasite growth.

925

926 All mosquito transmission experiments were performed using *Anopheles stephensi*
927 mosquitoes were housed in a temperature and humidity-controlled insectary at 24°C
928 and 70% humidity. Mosquito larvae were fed with mouse feed and yeast mixture and
929 adult mosquitoes were maintained on 10% glucose solution supplemented with
930 0.05% PABA.

931

932 **Parasite growth profiling**

933 For each isolate, an inoculum containing 1×10^6 parasitized RBCs was injected
934 intravenously to five CBA mice. Blood smears, haematocrit readings (Beckman
935 Coulter Counter) and body weight readings were taken daily for 20 days or until host
936 mortality to monitor parasitaemia, anaemia and weight loss. Blood smears were fixed
937 with 100% methanol and stained with Geimsa's solution. The average parasitaemia
938 was calculated from parasite and total RBC counts taken at three independent
939 microscopic fields.

940

941 **Genomic DNA isolation and whole genome sequencing**

942 Parasitized whole blood was collected from the brachial arteries of infected mice and
943 blood sera was removed by centrifugation. RBC pellets were washed once with PBS
944 and leukocyte-depleted using CF11 (Sigma Cat# C6288) cellulose columns. Parasite

945 pellets were obtained by gentle lysis of RBCs with 0.15% saponin solution. Genomic
946 DNA extraction from the parasite pellet was performed using DNAzol reagent
947 (Invitrogen CAT # 10503027) as per manufacturer's instructions.

948

949 Single-molecule sequencing was performed for five *P. vinckei* isolates. 5-10 ug of
950 gDNA was sheared using a Covaris g-TUBE shearing device to obtain target sizes of
951 20kB (for *Pv*CY, *Pv*bDA and *Pv*pCR) and 10kB (for samples *Pv*DE and *Pv*sEL).
952 Sheared DNA was concentrated using AMPure magnetic beads and SMRTbell
953 template libraries were generated as per Pacific Biosciences instructions. Libraries
954 were sequenced using P6 polymerase and chemistry version 4 (P6C4) on 3-6 SMRT
955 cells and sequenced on a PacBio RS II. Reads were filtered using SMRT portal v2.2
956 with default parameters. Read yields were 352,693, 356,960, 765,596, 386,746 and
957 675,879 reads for *Pv*CY, *Pv*bDA, *Pv*DE, *Pv*pCR and *Pv*sEL respectively totalling
958 around 2.7 to 4.7 Gb per sample. Mean subread lengths ranged from 6.15 to 9.1 kB.
959 N50 of 11.7 kB and 19.2 kB were obtained for 10 and 20 kB libraries respectively.

960

961 PCR-free Illumina sequencing was performed for all RMP isolates. 1-2 ug of DNA
962 was sheared using Covaris E series to obtain fragment sizes of 350 and 550bp.
963 350bp and 550bp PCR-free libraries were prepared using TruSeq PCR-free DNA
964 library preparation kits according to the manufacturer's instructions. Libraries were
965 sequenced on the Illumina HiSeq2000 platform with 2 X 100bp paired-end read
966 chemistry. Read yields ranged from 8-22 million reads for each library (see
967 Additional File 1).

968

969 **Genome assembly and annotation**

970 Genome assembly from long single molecule sequencing reads was performed
971 using FALCON (v0.2.1)[67] with length cutoff for seed reads used for initial mapping
972 set as
973 2,000bp and for pre-assembly set as 12,000bp. The falcon sense options were set
974 as- "--min idt 0.70 --min cov 4 --local match count threshold 2 --max n read 200"
975 and overlap filtering settings were set as "--max diff 240 --max cov 360 --min cov
976 5 --bestn 10". 28-40 unitigs were obtained and smaller unitigs were discarded as
977 they were exact copies of the regions already present in the larger unitigs.

978

979 PCR-free reads were used to correct base call errors in the unitigs using ICORN2
980 [68], run with default settings and for 15 iterations. The unitigs were classified as
981 chromosomes based on their homology with *P. chabaudi* chromosomes (GeneDB
982 version 3). In *Pv*DE and *Pvs*EL samples, some of the chromosomes were made of
983 two to three unitigs with overlapping ends which were then fused and the gaps were
984 removed manually. Apicoplast and mitochondrial genomes were assembled from
985 PCR-free reads alone using Velvet assembler [69].

986

987 Syntenic regions between genome sequences were identified using MUMmer v3.2
988 [70]. Synteny breakpoints were identified manually and were confirmed not to be
989 misassemblies by verifying that they had continuous read coverage from PacBio and
990 Illumina reads. Artemis Comparison tool [71, 72] and Integrative Genomics Viewer
991 [73] were used for this purpose. The structural variations were illustrated using
992 CIRCOS [74].

993 *De novo* gene predictions were made using AUGUSTUS [75] trained on *P. chabaudi*
994 gene models. RNA sequencing reads were mapped onto the reference genome

995 using TopHat [76] to infer splice junctions. AUGUSTUS predicted gene models,
996 junctions.bed file from TopHat and *P. chabaudi* gene models were fed into MAKER
997 [77] to create consensus gene models that were then manually curated based on
998 RNAseq evidence in Artemis Viewer and Artemis Comparison tool [71, 72].
999 Ribosomal RNA (rRNA) and transfer RNA (tRNA) were annotated using RNAmmer
1000 v1.2 [78]. Gene product calls were assigned to *P. vinckei* gene models based on
1001 above identified orthologous groups using custom scripts. Functional domain
1002 annotations were inferred from InterPro database using InterProScan v5.17 [79].
1003 Transmembrane domains were predicted by TMHMMv2.0 [80], signal peptide
1004 cleavage sites by SignalP v4.0 [81], presence of PEXEL/VTs motif detected using
1005 ExportPredv4.0 [82] (with PEXEL score cutoff of 4.3).

1006

1007 **Transcriptomics**

1008 Total RNA was isolated for four *P. vinckei* isolates (*PvbDA*, *PvpCR*, *PvIDS* and
1009 *PvsEL*) from mixed blood stages using TRIzol (Invitrogen) following the
1010 manufacturer's protocol. For *PvpCR* and *PvIDS*, additionally, total RNA was isolated
1011 from ring, trophozoite and gametocyte enriched fractions obtained using a Nycodenz
1012 gradient.

1013 Strand-specific mRNA sequencing was performed from total RNA using TruSeq
1014 Stranded mRNA Sample Prep Kit LT (Illumina) according to the manufacturer's
1015 instructions. Briefly, polyA+ mRNA was purified from total RNA using oligo-dT
1016 dynabead selection. First strand cDNA was synthesised using randomly primed
1017 oligos followed by second strand synthesis where dUTPs were incorporated to
1018 achieve strand-specificity. The cDNA was adapter-ligated and the libraries amplified

1019 by PCR. Libraries were sequenced in Illumina Hiseq2000 with paired-end 100bp
1020 read chemistry.

1021

1022 Stage-specific RNAseq data for *Pv*CY's intraerythrocytic growth stages were
1023 obtained from an earlier study [50]. Gene expression was captured every 6 hours
1024 during *Pv*CY's 24 h IDC with three replicates, of which 6h, 12h and 24h timepoints
1025 were used in this study to denote gene expression at ring, trophozoite and schizont
1026 stages respectively. Similarly, for *P. chabaudi* AS, gene expression was captured
1027 every 3h during its IDC with two replicates in a recent study [56], of which the 5.5h,
1028 11.5h and 23.5 h timepoints on day 2 were chosen to denote ring, trophozoite and
1029 schizont stages respectively. *P. yoelii* and *P. berghei* transcriptome data were
1030 obtained from [26] and [44] respectively.

1031

1032 **SNP calling and molecular evolution analysis**

1033 Illumina paired-end reads for a total of 30 RMP isolates produced in this study or
1034 sourced from previous studies (see Additional File 13) were used for SNP calling. In
1035 the case of isolates sequenced in this study, the 350bp fragment size PCR-free
1036 sequencing data was used. First, to produce a high quality pan-RMP SNP dataset
1037 for phylogeny construction, all quality-trimmed reads were mapped onto the *Pv*CY
1038 reference genome using BWA tool [83] with default parameters. MAPQ values of the
1039 mapped reads were fixed and duplicated reads removed using CleanSam,
1040 FixMateInformation and MarkDuplicates commands in picardtools
1041 (<http://broadinstitute.github.io/picard>) and only uniquely mapped reads were retained
1042 using samtools with parameter -q 1 (<http://www.htslib.org/>). Raw SNPs were called
1043 from the mapped reads using samtools mpileup and bcftools with following

1044 parameters- minimum base quality of 20, minimum mapping quality of 10 and ploidy
1045 of 1. SNPs with quality (QUAL) less than 20, read depth (DP) less than 10, mapping
1046 quality (MQ) less than 2 and allele frequency (AF1) less than 80% were removed.
1047 Further, only SNPs present in protein-coding genes were retained and those present
1048 in low-complexity regions (predicted by DustMasker [84]) and sub-telomeric
1049 multigene family members were excluded.

1050

1051 The filtered SNPs from different samples were merged and SNP positions with
1052 missing calls in more than six samples were removed. This filtered high-quality set of
1053 1,020,956 SNP positions were used to infer maximum likelihood phylogeny (see
1054 Additional File 7).

1055

1056 For inferring Ka/Ks ratios between *P. vinckei* isolates and *PvvcY*, filtered SNPs
1057 obtained above were merged as before but excluding *PvpBS* due to its high missing
1058 call rate. Only SNP positions with no missing calls in any sample were retained and
1059 morphed onto *PvvcY* gene sequences using gatk command
1060 FastaAlternateReferenceMaker [85] to produce isolate-specific gene sequences
1061 which were then used for pairwise sequence comparisons to identify synonymous
1062 and non-synonymous substitutions. Ka/Ks ratios were calculated using KaKs
1063 Calculator [86] and averaged across isolates if more than one was available for a
1064 subspecies.

1065

1066 For comparisons against *P. v. petteri*, *P. yoelii* and *P. chabaudi*, sample reads were
1067 mapped onto *PvpCR*, *P. yoelii* 17X and *P. chabaudi* AS genomes respectively and

1068 subsequent steps were followed as before. Similar to *PvpBS*, *PysEL* was excluded
1069 from Ka/Ks analysis due to high missing rate.

1070

1071 **Phylogenetic analysis**

1072 For constructing species-level phylogenies, orthologous proteins were identified
1073 between the five *P. vinckei* genomes, three RMP genomes, *P. falciparum*, *P.*
1074 *knowlesi* and *P. vivax* genomes using OrthoMCL v2.0.9 [87] with inflation parameter
1075 as 1.5, BLAST hit evaluate cutoff as $1e^{-5}$ and percentage match cutoff as 50%.

1076

1077 One-to-one orthologous proteins from each of the 3,920 ortholog groups that form
1078 the core proteome were aligned using MUSCLE [88]. Alignments were trimmed
1079 using trimAl [89] removing all gaps and concatenated into a partitioned alignment
1080 using catsequence. An initial RAxML [90] run was performed on individual
1081 alignments to identify best amino acid substitution model under the Akaike
1082 Information Criterion (--auto-prot=aic). These models were then used to run a
1083 partitioned RAxML analysis on the concatenated protein alignment using
1084 PROT GAMMA model for rate heterogeneity.

1085

1086 For constructing isolate-level phylogeny, the vcf files containing high-quality SNPs
1087 were first converted to a matrix for phylogenetic analysis using vcf2phylip
1088 (<https://github.com/edgardomortiz/vcf2phylip>). RAxML tree inference was performed
1089 using GTR GAMMA model for rate heterogeneity along with ascertainment bias
1090 correction (--asc-corr=stamatakis) since we used only variant sites.

1091

1092 Maximum likelihood trees for multigene families were constructed based on
1093 nucleotide sequence alignments of member genes that included intron sequences if
1094 present (except in the case of *pir* family where introns were excluded). Alignments
1095 were performed using MUSCLE with default parameters, frame-shifts edited
1096 manually in AliView [91] followed by automated trimming with trimAl using -gappyout
1097 parameter. In all the phylogenies, bootstrapping was conducted until the majority-
1098 rule consensus tree criterion (-l autoMRE) was satisfied (usually 150-300 replicates).
1099 Phylogenetic trees were visualized and annotated in the iTOL server [66].

1100

1101 **Plasmid construction and transfection in *P. vinckei***

1102 The pPvCY-p230p-gfpLuc plasmid was constructed using MultiSite Gateway
1103 cloning
1104 system (Invitrogen). attB-flanked 5'and 3'homology arms were obtained by
1105 amplifying
1106 800bp regions upstream and downstream of PVVCY_0300700. These fragments
1107 were subjected to independent BP recombination with pDONRP4-P1R (Invitrogen) to
1108 generate entry plasmids pENT12-5U and pENT41-3U, respectively. Similarly, the
1109 gfpLuc cassette from pL1063 was amplified and subjected to LR reaction to obtain
1110 pENT23-gfpLuc. BP reaction was performed using the BP Clonase II enzyme mix
1111 (Invitrogen) according to the manufacturer's instructions.

1112

1113 *Plasmodium vinckei vinckei* CY schizont-enriched fraction was collected by
1114 differential centrifugation on 50% Nycodenz in incomplete RPMI1640 medium, and
1115 20 ug of ApaI- and StuI-double digested linearized transfection constructs were
1116 electroporated to 1×10^7 of enriched schizonts using a Nucleofector device (Amaxa)

1117 with human T-cell solution under program U-33. Transfected parasites were
1118 intravenously injected into
1119 7-week-old ICR female mice, which were treated by administering pyrimethamine in
1120 the drinking water (0.07 mg/mL) 24 hours later for a period of 4-7 days. Drug
1121 resistant parasites were cloned by limiting dilution with an inoculum of 0.3
1122 parasites/100 μ L injected into 10 female ICR mice. Two clones were obtained, and
1123 integration of the transfection constructs was confirmed by PCR amplification with a
1124 unique set of primers for the modified p230p gene locus. Live imaging of parasites
1125 was performed on thin smears of parasite-infected blood prepared on glass slides
1126 stained with Hoechst 33342. Fluorescent and differential interference contrast (DIC)
1127 images were captured using an AxioCam MRm CCD camera (Carl Zeiss, Germany)
1128 fixed to an Axio imager Z2 fluorescent microscope with a Plan-Apochromat 100 \times /1.4
1129 oil immersion lens (Carl Zeiss) and Axiovision software (Carl Zeiss). GFP-expressing
1130 *P. vinckei* oocysts in mosquito midguts were imaged in SMZ25 microscope (Nikon).

1131

1132 **Mosquito transmission and genetic crossing of *P. vinckei* parasites**

1133 To determine the optimal transmission temperature for *P. vinckei baforti* isolates,
1134 infected CBA mice were anaesthetized on day 3 post-inoculation and ~100 female
1135 *Anopheles stephensi* mosquitoes (7 to 12 days post emergence) were allowed to
1136 take a blood meal for 30 min without interruption after confirming presence of
1137 gametocytes by microscopy. Three batches of ~100 mosquitoes were fed at three
1138 different temperatures - 21°C, 23°C and 26°C. The fed mosquitoes were maintained
1139 at the feed temperatures and at 70% humidity. To check for presence of
1140 oocysts/sporozites, mosquitoes were dissected, and their midguts or salivary

1141 glands were suspended in a drop of PBS solution atop a glass slide, covered by a
1142 coverslip and studied under a microscope.

1143

1144 For genetic crossing, isolates were harvested from donor mice and mixed to achieve
1145 a 1:1 ratio and 1×10^6 parasites of this mixture was inoculated into four female CBA
1146 mice. Three days after inoculation, after confirming the presence of gametocytes,
1147 two infected CBA mice were anaesthetized and placed on two mosquito cages, each
1148 containing around 80 mosquitoes each. Mosquitoes were allowed to feed on the
1149 mice without interruption for 40 minutes at 24°C. A fresh feed was again performed
1150 on the 4th day post-inoculation with the other two CBA mice and two fresh cages of
1151 mosquitoes. 5-10 female mosquitoes from each cage were dissected on the 9th and
1152 12th day after the blood meal to check for presence of oocysts in the mosquito
1153 midguts. Twenty days after the blood meal, the mosquitoes were dissected and the
1154 salivary glands were removed, placed in 0.5-0.7 ml PBS solution and gently
1155 disrupted

1156 to release sporozoites. The suspensions from day 3 and day 4 feeds were injected
1157 intravenously into an ICR mouse each. When the mice were positive for blood-stage
1158 parasites, they were sub-inoculated into ten ICR mice with an inoculum of 0.6
1159 parasites/100uL to obtain clones from the potential cross progeny by limiting dilution.
1160 Eight days post infection, four mice were positive for parasites and these clones
1161 were screened for the presence of both *PvsEH* and *PvsEL* alleles within the
1162 chromosomes.

1163

1164 **Declarations**

1165 **Ethics approval and consent to participate**

1166 Laboratory animal experimentation was performed in strict accordance with the
1167 Japanese Humane Treatment and Management of Animals Law (Law No. 105 dated
1168 19 October 1973 modified on 2 June 2006), and the Regulation on Animal
1169 Experimentation at Nagasaki University, Japan. The protocol was approved by the
1170 Institutional Animal Research Committee of Nagasaki University (permit:
1171 12072610052).

1172

1173 **Consent for publication**

1174 Not applicable

1175 **Availability of data and materials**

1176 All genome sequences, gene annotations and sequencing data files generated in
1177 this study can be found in ENA Study: PRJEB19355. All the datasets would also be
1178 available via EuPathDB portal at the time of publication. All parasite resources will be
1179 made available to the scientific community via the BEI Resources
1180 (<https://www.beiresources.org/>). Searchable and interactive versions of the
1181 phylogeny trees produced in this study can be accessed at
1182 <https://itol.embl.de/shared/2ICr6w0mdDENs>.

1183 **Competing interests**

1184 The authors declare that they have no competing interests.

1185

1186 **Funding**

1187 RC was supported by a Grant (JP16K21233) from the Japan Society for the
1188 Promotion of Science. This work was supported by KAUST faculty baseline fund
1189 (BAS/1/1020-01-01) and Competitive Research Fund (URF/1/2267-01-01) to AP.

1190

1191 **Authors' contributions**

1192 RC and AP conceived the study. AR and RC conducted all rodent and mosquito
1193 experiments. AR and OG prepared sequencing libraries. AR, SK and RC conducted
1194 genetic cross experiments. AR collected data and performed all bioinformatic
1195 analyses. AR wrote the manuscript and all authors contributed to it.

1196

1197 **Acknowledgements**

1198 The authors would like to acknowledge the personnel at the Bioscience Core
1199 Laboratory (BCL) at King Abdullah University of Science and Technology for their
1200 help with next generation sequencing. We acknowledge the contribution of Professor
1201 Richard Carter, whose support of this work was crucial to its inception and
1202 completion.

1203

1204 **Authors' information (optional)**

1205 Not applicable.

1206

1207 **References**

- 1208 1. Carlton JM, Hayton K, Cravo PV, Walliker D: **Of mice and malaria mutants:
1209 unravelling the genetics of drug resistance using rodent malaria models.** *Trends
1210 Parasitol* 2001, **17**(5):236-242.
- 1211 2. Culleton RL, Abkallo HM: **Malaria parasite genetics: doing something useful.**
1212 *Parasitol Int* 2015, **64**(3):244-253.
- 1213 3. Matz JM, Kooij TW: **Towards genome-wide experimental genetics in the in vivo
1214 malaria model parasite Plasmodium berghei.** *Pathog Glob Health* 2015, **109**(2):46-
1215 60.
- 1216 4. De Niz M, Heussler VT: **Rodent malaria models: insights into human disease and
1217 parasite biology.** *Curr Opin Microbiol* 2018, **46**:93-101.
- 1218 5. Carter R: **Studies on enzyme variation in the murine malaria parasites Plasmodium
1219 berghei, P. yoelii, P. vinckei and P. chabaudi by starch gel electrophoresis.**
1220 *Parasitology* 1978, **76**(3):241-267.

- 1221 6. Perkins SL, Sarkar IN, Carter R: **The phylogeny of rodent malaria parasites:**
1222 **simultaneous analysis across three genomes.** *Infect Genet Evol* 2007, **7**(1):74-83.
- 1223 7. Ramiro RS, Reece SE, Obbard DJ: **Molecular evolution and phylogenetics of rodent**
1224 **malaria parasites.** *BMC Evol Biol* 2012, **12**:219.
- 1225 8. Cravo PV, Carlton JM, Hunt P, Bisoni L, Padua RA, Walliker D: **Genetics of mefloquine**
1226 **resistance in the rodent malaria parasite Plasmodium chabaudi.** *Antimicrob Agents*
1227 *Chemother* 2003, **47**(2):709-718.
- 1228 9. Langhorne J, Quin SJ, Sanni LA: **Mouse models of blood-stage malaria infections:**
1229 **immune responses and cytokines involved in protection and pathology.** *Chem*
1230 *Immunol* 2002, **80**:204-228.
- 1231 10. Spence PJ, Jarra W, Levy P, Reid AJ, Chappell L, Brugat T, Sanders M, Berriman M,
1232 Langhorne J: **Vector transmission regulates immune control of Plasmodium**
1233 **virulence.** *Nature* 2013, **498**(7453):228-231.
- 1234 11. Brugat T, Reid AJ, Lin J, Cunningham D, Tumwine I, Kushinga G, McLaughlin S, Spence
1235 P, Bohme U, Sanders M *et al*: **Antibody-independent mechanisms regulate the**
1236 **establishment of chronic Plasmodium infection.** *Nat Microbiol* 2017, **2**:16276.
- 1237 12. Stephens R, Culleton RL, Lamb TJ: **The contribution of Plasmodium chabaudi to our**
1238 **understanding of malaria.** *Trends Parasitol* 2012, **28**(2):73-82.
- 1239 13. Prudencio M, Mota MM, Mendes AM: **A toolbox to study liver stage malaria.** *Trends*
1240 *Parasitol* 2011, **27**(12):565-574.
- 1241 14. Guttery DS, Roques M, Holder AA, Tewari R: **Commit and Transmit: Molecular**
1242 **Players in Plasmodium Sexual Development and Zygote Differentiation.** *Trends*
1243 *Parasitol* 2015, **31**(12):676-685.
- 1244 15. Pfander C, Anar B, Schwach F, Otto TD, Brochet M, Volkmann K, Quail MA, Pain A,
1245 Rosen B, Skarnes W *et al*: **A scalable pipeline for highly effective genetic**
1246 **modification of a malaria parasite.** *Nat Methods* 2011, **8**(12):1078-1082.
- 1247 16. Marr E, Milne R, Anar B, Girling G, Schwach F, Mooney J, Nahrendorf W, Spence P,
1248 Cunningham D, Baker D *et al*: **An enhanced toolkit for the generation of knockout**
1249 **and marker-free fluorescent Plasmodium chabaudi [version 1; peer review: 2**
1250 **approved].** *Wellcome Open Research* 2020, **5**(71).
- 1251 17. Janse CJ, Ramesar J, Waters AP: **High-efficiency transfection and drug selection of**
1252 **genetically transformed blood stages of the rodent malaria parasite Plasmodium**
1253 **berghei.** *Nat Protoc* 2006, **1**(1):346-356.
- 1254 18. Jongco AM, Ting LM, Thathy V, Mota MM, Kim K: **Improved transfection and new**
1255 **selectable markers for the rodent malaria parasite Plasmodium yoelii.** *Mol Biochem*
1256 *Parasitol* 2006, **146**(2):242-250.
- 1257 19. Bushell E, Gomes AR, Sanderson T, Anar B, Girling G, Herd C, Metcalf T, Modrzynska
1258 K, Schwach F, Martin RE *et al*: **Functional Profiling of a Plasmodium Genome**
1259 **Reveals an Abundance of Essential Genes.** *Cell* 2017, **170**(2):260-272 e268.
- 1260 20. Stanway RR, Bushell E, Chiappino-Pepe A, Roques M, Sanderson T, Franke-Fayard B,
1261 Caldelari R, Golomingi M, Nyonda M, Pandey V *et al*: **Genome-Scale Identification of**
1262 **Essential Metabolic Processes for Targeting the Plasmodium Liver Stage.** *Cell* 2019,
1263 **179**(5):1112-1128 e1126.
- 1264 21. Antonova-Koch Y, Meister S, Abraham M, Luth MR, Ottilie S, Lukens AK, Sakata-Kato
1265 T, Vanaerschot M, Owen E, Jado JC *et al*: **Open-source discovery of chemical leads**
1266 **for next-generation chemoprotective antimalarials.** *Science* 2018, **362**(6419).

- 1267 22. de Koning-Ward TF, Gilson PR, Crabb BS: **Advances in molecular genetic systems in**
1268 **malaria.** *Nat Rev Microbiol* 2015, **13**(6):373-387.
- 1269 23. Carlton JM, Angiuoli SV, Suh BB, Kooij TW, Perteu M, Silva JC, Ermolaeva MD, Allen JE,
1270 Selengut JD, Koo HL *et al*: **Genome sequence and comparative analysis of the model**
1271 **rodent malaria parasite Plasmodium yoelii yoelii.** *Nature* 2002, **419**(6906):512-519.
- 1272 24. Hall N, Karras M, Raine JD, Carlton JM, Kooij TW, Berriman M, Florens L, Janssen CS,
1273 Pain A, Christophides GK *et al*: **A comprehensive survey of the Plasmodium life cycle**
1274 **by genomic, transcriptomic, and proteomic analyses.** *Science* 2005, **307**(5706):82-
1275 86.
- 1276 25. Fougere A, Jackson AP, Bechtesi DP, Braks JA, Annoura T, Fonager J, Spaccapelo R,
1277 Ramesar J, Chevalley-Maurel S, Klop O *et al*: **Variant Exported Blood-Stage Proteins**
1278 **Encoded by Plasmodium Multigene Families Are Expressed in Liver Stages Where**
1279 **They Are Exported into the Parasitophorous Vacuole.** *PLoS Pathog* 2016,
1280 **12**(11):e1005917.
- 1281 26. Otto TD, Bohme U, Jackson AP, Hunt M, Franke-Fayard B, Hoeijmakers WA, Religa AA,
1282 Robertson L, Sanders M, Ogun SA *et al*: **A comprehensive evaluation of rodent**
1283 **malaria parasite genomes and gene expression.** *BMC Biol* 2014, **12**:86.
- 1284 27. Bafort JM: **The biology of rodent malaria with particular reference to Plasmodium**
1285 **vinckei vinckei Rodhain 1952.** *Ann Soc Belges Med Trop Parasitol Mycol* 1971,
1286 **51**(1):5-203.
- 1287 28. Carter R, Walliker D: **New observations on the malaria parasites of rodents of the**
1288 **Central African Republic - Plasmodium vinckei petteri subsp. nov. and Plasmodium**
1289 **chabaudi Landau, 1965.** *Ann Trop Med Parasitol* 1975, **69**(2):187-196.
- 1290 29. Carter R, Walliker D: **Malaria parasites of rodents of the Congo (Brazzaville):**
1291 **Plasmodium chabaudi adami subsp. nov. and Plasmodium vinckei lentum Landau,**
1292 **Michel, Adam and Boulard, 1970.** *Ann Parasitol Hum Comp* 1976, **51**(6):637-646.
- 1293 30. Killick-Kendrick R: **Parasitic Protozoa of the blood of rodents. V. Plasmodium**
1294 **vinckei brucechwatti subsp. nov. A malaria parasite of the thicket rat, Thamnomys**
1295 **rutilans, in Nigeria.** *Ann Parasitol Hum Comp* 1975, **50**(3):251-264.
- 1296 31. Landau I, Michel JC, Adam JP, Boulard Y: **The life cycle of Plasmodium vinckei**
1297 **lentum subsp. nov. in the laboratory; comments on the nomenclature of the**
1298 **murine malaria parasites.** *Ann Trop Med Parasitol* 1970, **64**(3):315-323.
- 1299 32. Bafort J: **New isolations of murine malaria in Africa: Cameroon.** In: *5th International*
1300 *Congress of Protozoology, New York City Abstracts of papers p343: 1977.*
- 1301 33. Bafort J: **Etude du cycle biologique du Plasmodium v. vinckei Rodhain 1952.** *Ann*
1302 *Soc Belge Méd Trop* 1969, **49**(6):533-628.
- 1303 34. Bafort JM, Molyneux DH: **Liver infections with Plasmodium v. vinckei in hosts**
1304 **refractory to blood infection.** *Trans R Soc Trop Med Hyg* 1971, **65**(1):13.
- 1305 35. Lainson FA: **Observations on the morphology and electrophoretic variation of**
1306 **enzymes of the rodent malaria parasites of Cameroon, Plasmodium yoelii, P.**
1307 **chabaudi and P. vinckei.** *Parasitology* 1983, **86** (Pt 2):221-229.
- 1308 36. Carter R: **Enzyme variation in Plasmodium berghei and Plasmodium vinckei.**
1309 *Parasitology* 1973, **66**(2):297-307.
- 1310 37. LaCrue AN, Scheel M, Kennedy K, Kumar N, Kyle DE: **Effects of artesunate on**
1311 **parasite recrudescence and dormancy in the rodent malaria model Plasmodium**
1312 **vinckei.** *PLoS One* 2011, **6**(10):e26689.

- 1313 38. Gautret P, Deharo E, Chabaud AG, Ginsburg H, Landau I: **Plasmodium vinckei vinckei,**
1314 **P. v. lentum and P. yoelii yoelii: chronobiology of the asexual cycle in the blood.**
1315 *Parasite* 1994, **1**(3):235-239.
- 1316 39. Chandra R, Kumar S, Puri SK: **Plasmodium vinckei: infectivity of arteether-sensitive**
1317 **and arteether-resistant parasites in different strains of mice.** *Parasitol Res* 2011,
1318 **109**(4):1143-1149.
- 1319 40. Killick-Kendrick R, Peters W: **Rodent malaria.** London: Academic Press; 1978.
- 1320 41. Kooij TW, Carlton JM, Bidwell SL, Hall N, Ramesar J, Janse CJ, Waters AP: **A**
1321 **Plasmodium whole-genome synteny map: indels and synteny breakpoints as foci**
1322 **for species-specific genes.** *PLoS Pathog* 2005, **1**(4):e44.
- 1323 42. Carlton J, Angiuoli S, Suh B, Kooij T, Perteza M, Silva J, Ermolaeva M, Allen J, Selengut
1324 J, Koo H *et al*: **Genome sequence and comparative analysis of the model rodent**
1325 **malaria parasite Plasmodium yoelii yoelii.** *Nature* 2002, **419**(6906):512-519.
- 1326 43. Liu SL, Sanderson KE: **Rearrangements in the genome of the bacterium Salmonella**
1327 **typhi.** *Proc Natl Acad Sci U S A* 1995, **92**(4):1018-1022.
- 1328 44. Abkallo HM, Martinelli A, Inoue M, Ramaprasad A, Xangsayarath P, Gitaka J, Tang J,
1329 Yahata K, Zoungrana A, Mitaka H *et al*: **Rapid identification of genes controlling**
1330 **virulence and immunity in malaria parasites.** *PLoS Pathog* 2017, **13**(7):e1006447.
- 1331 45. Akinosoglou KA, Bushell ES, Ukegbu CV, Schlegelmilch T, Cho JS, Redmond S, Sala K,
1332 Christophides GK, Vlachou D: **Characterization of Plasmodium developmental**
1333 **transcriptomes in Anopheles gambiae midgut reveals novel regulators of malaria**
1334 **transmission.** *Cell Microbiol* 2015, **17**(2):254-268.
- 1335 46. Ukegbu CV, Giorgalli M, Tapanelli S, Rona LDP, Jaye A, Wyer C, Angrisano F,
1336 Blagborough AM, Christophides GK, Vlachou D: **PIMMS43 is required for malaria**
1337 **parasite immune evasion and sporogonic development in the mosquito vector.**
1338 *Proc Natl Acad Sci U S A* 2020, **117**(13):7363-7373.
- 1339 47. Sultan AA, Thathy V, Frevert U, Robson KJ, Crisanti A, Nussenzweig V, Nussenzweig
1340 RS, Menard R: **TRAP is necessary for gliding motility and infectivity of plasmodium**
1341 **sporozoites.** *Cell* 1997, **90**(3):511-522.
- 1342 48. Sanders PR, Gilson PR, Cantin GT, Greenbaum DC, Nebl T, Carucci DJ, McConville MJ,
1343 Schofield L, Hodder AN, Yates JR, 3rd *et al*: **Distinct protein classes including novel**
1344 **merozoite surface antigens in Raft-like membranes of Plasmodium falciparum.** *J*
1345 *Biol Chem* 2005, **280**(48):40169-40176.
- 1346 49. Taechalerpaisarn T, Crosnier C, Bartholdson SJ, Hodder AN, Thompson J,
1347 Bustamante LY, Wilson DW, Sanders PR, Wright GJ, Rayner JC *et al*: **Biochemical and**
1348 **functional analysis of two Plasmodium falciparum blood-stage 6-cys proteins: P12**
1349 **and P41.** *PLoS One* 2012, **7**(7):e41937.
- 1350 50. Ramaprasad A, Subudhi AK, Culleton R, Pain A: **A fast and cost-effective**
1351 **microsampling protocol incorporating reduced animal usage for time-series**
1352 **transcriptomics in rodent malaria parasites.** *Malar J* 2019, **18**(1):26.
- 1353 51. Favaloro JM, Kemp DJ: **Sequence diversity of the erythrocyte membrane antigen 1**
1354 **in various strains of Plasmodium chabaudi.** *Mol Biochem Parasitol* 1994, **66**(1):39-
1355 47.
- 1356 52. Miller JL, Murray S, Vaughan AM, Harupa A, Sack B, Baldwin M, Crispe IN, Kappe SH:
1357 **Quantitative bioluminescent imaging of pre-erythrocytic malaria parasite infection**
1358 **using luciferase-expressing Plasmodium yoelii.** *PLoS One* 2013, **8**(4):e60820.

- 1359 53. Franke-Fayard B, Trueman H, Ramesar J, Mendoza J, van der Keur M, van der Linden
1360 R, Sinden RE, Waters AP, Janse CJ: **A Plasmodium berghei reference line that**
1361 **constitutively expresses GFP at a high level throughout the complete life cycle.** *Mol*
1362 *Biochem Parasitol* 2004, **137**(1):23-33.
- 1363 54. Boundenga L, Ngoubangoye B, Ntie S, Moukodoum ND, Renaud F, Rougeron V,
1364 Prugnolle F: **Rodent malaria in Gabon: Diversity and host range.** *Int J Parasitol*
1365 *Parasites Wildl* 2019, **10**:117-124.
- 1366 55. Palmer GH, Brayton KA: **Gene conversion is a convergent strategy for pathogen**
1367 **antigenic variation.** *Trends Parasitol* 2007, **23**(9):408-413.
- 1368 56. Subudhi AK, O'Donnell AJ, Ramaprasad A, Abkallo HM, Kaushik A, Ansari HR, Abdel-
1369 Haleem AM, Ben Rached F, Kaneko O, Culleton R *et al*: **Malaria parasites regulate**
1370 **intra-erythrocytic development duration via serpentine receptor 10 to coordinate**
1371 **with host rhythms.** *Nat Commun* 2020, **11**(1):2763.
- 1372 57. Voza T, Gautret P, Renia L, Gantier JC, Lombard MN, Chabaud AG, Landau I:
1373 **Variation in murid Plasmodium desequestration and its modulation by stress and**
1374 **pentoxifylline.** *Parasitol Res* 2002, **88**(4):344-349.
- 1375 58. Clark IA, Cowden WB, Butcher GA, Hunt NH: **Possible roles of tumor necrosis factor**
1376 **in the pathology of malaria.** *Am J Pathol* 1987, **129**(1):192-199.
- 1377 59. Yoeli M, Hargreaves BJ: **Brain capillary blockage produced by a virulent strain of**
1378 **rodent malaria.** *Science* 1974, **184**(4136):572-573.
- 1379 60. Tang J, Templeton TJ, Cao J, Culleton R: **The Consequences of Mixed-Species Malaria**
1380 **Parasite Co-Infections in Mice and Mosquitoes for Disease Severity, Parasite**
1381 **Fitness, and Transmission Success.** *Front Immunol* 2019, **10**:3072.
- 1382 61. Abkallo HM, Tangena JA, Tang J, Kobayashi N, Inoue M, Zoungrana A, Colegrave N,
1383 Culleton R: **Within-host competition does not select for virulence in malaria**
1384 **parasites; studies with Plasmodium yoelii.** *PLoS Pathog* 2015, **11**(2):e1004628.
- 1385 62. Martinelli A, Cheesman S, Hunt P, Culleton R, Raza A, Mackinnon M, Carter R: **A**
1386 **genetic approach to the de novo identification of targets of strain-specific**
1387 **immunity in malaria parasites.** *Proc Natl Acad Sci U S A* 2005, **102**(3):814-819.
- 1388 63. Culleton R, Martinelli A, Hunt P, Carter R: **Linkage group selection: rapid gene**
1389 **discovery in malaria parasites.** *Genome Res* 2005, **15**(1):92-97.
- 1390 64. Pattaradilokrat S, Culleton RL, Cheesman SJ, Carter R: **Gene encoding erythrocyte**
1391 **binding ligand linked to blood stage multiplication rate phenotype in Plasmodium**
1392 **yoelii yoelii.** *Proc Natl Acad Sci U S A* 2009, **106**(17):7161-7166.
- 1393 65. Knowles G, Sanderson A, Walliker D: **Plasmodium yoelii: genetic analysis of crosses**
1394 **between two rodent malaria subspecies.** *Exp Parasitol* 1981, **52**(2):243-247.
- 1395 66. Letunic I, Bork P: **Interactive Tree Of Life (iTOL) v4: recent updates and new**
1396 **developments.** *Nucleic Acids Res* 2019, **47**(W1):W256-W259.
- 1397 67. Chin CS, Peluso P, Sedlazeck FJ, Nattestad M, Concepcion GT, Clum A, Dunn C,
1398 O'Malley R, Figueroa-Balderas R, Morales-Cruz A *et al*: **Phased diploid genome**
1399 **assembly with single-molecule real-time sequencing.** *Nat Methods* 2016,
1400 **13**(12):1050-1054.
- 1401 68. Otto TD, Sanders M, Berriman M, Newbold C: **Iterative Correction of Reference**
1402 **Nucleotides (iCORN) using second generation sequencing technology.**
1403 *Bioinformatics* 2010, **26**(14):1704-1707.
- 1404 69. Zerbino DR, Birney E: **Velvet: algorithms for de novo short read assembly using de**
1405 **Brujin graphs.** *Genome Res* 2008, **18**(5):821-829.

- 1406 70. Kurtz S, Phillippy A, Delcher AL, Smoot M, Shumway M, Antonescu C, Salzberg SL:
1407 **Versatile and open software for comparing large genomes.** *Genome Biol* 2004,
1408 5(2):R12.
- 1409 71. Carver T, Harris SR, Berriman M, Parkhill J, McQuillan JA: **Artemis: an integrated**
1410 **platform for visualization and analysis of high-throughput sequence-based**
1411 **experimental data.** *Bioinformatics* 2012, **28**(4):464-469.
- 1412 72. Carver TJ, Rutherford KM, Berriman M, Rajandream MA, Barrell BG, Parkhill J: **ACT:**
1413 **the Artemis Comparison Tool.** *Bioinformatics* 2005, **21**(16):3422-3423.
- 1414 73. Robinson JT, Thorvaldsdottir H, Winckler W, Guttman M, Lander ES, Getz G, Mesirov
1415 JP: **Integrative genomics viewer.** *Nat Biotechnol* 2011, **29**(1):24-26.
- 1416 74. Krzywinski M, Schein J, Birol I, Connors J, Gascoyne R, Horsman D, Jones SJ, Marra
1417 MA: **Circos: an information aesthetic for comparative genomics.** *Genome Res* 2009,
1418 **19**(9):1639-1645.
- 1419 75. Stanke M, Waack S: **Gene prediction with a hidden Markov model and a new intron**
1420 **submodel.** *Bioinformatics* 2003, **19 Suppl 2**:ii215-225.
- 1421 76. Kim D, Pertea G, Trapnell C, Pimentel H, Kelley R, Salzberg SL: **TopHat2: accurate**
1422 **alignment of transcriptomes in the presence of insertions, deletions and gene**
1423 **fusions.** *Genome Biol* 2013, **14**(4):R36.
- 1424 77. Campbell MS, Holt C, Moore B, Yandell M: **Genome Annotation and Curation Using**
1425 **MAKER and MAKER-P.** *Curr Protoc Bioinformatics* 2014, **48**:4 11 11-14 11 39.
- 1426 78. Lagesen K, Hallin P, Rodland EA, Staerfeldt HH, Rognes T, Ussery DW: **RNAmmer:**
1427 **consistent and rapid annotation of ribosomal RNA genes.** *Nucleic Acids Res* 2007,
1428 **35**(9):3100-3108.
- 1429 79. Jones P, Binns D, Chang HY, Fraser M, Li W, McAnulla C, McWilliam H, Maslen J,
1430 Mitchell A, Nuka G *et al*: **InterProScan 5: genome-scale protein function**
1431 **classification.** *Bioinformatics* 2014, **30**(9):1236-1240.
- 1432 80. Krogh A, Larsson B, von Heijne G, Sonnhammer EL: **Predicting transmembrane**
1433 **protein topology with a hidden Markov model: application to complete genomes.** *J*
1434 *Mol Biol* 2001, **305**(3):567-580.
- 1435 81. Petersen TN, Brunak S, von Heijne G, Nielsen H: **SignalP 4.0: discriminating signal**
1436 **peptides from transmembrane regions.** *Nat Methods* 2011, **8**(10):785-786.
- 1437 82. Sargeant TJ, Marti M, Caler E, Carlton JM, Simpson K, Speed TP, Cowman AF:
1438 **Lineage-specific expansion of proteins exported to erythrocytes in malaria**
1439 **parasites.** *Genome Biol* 2006, **7**(2):R12.
- 1440 83. Li H, Durbin R: **Fast and accurate short read alignment with Burrows-Wheeler**
1441 **transform.** *Bioinformatics* 2009, **25**(14):1754-1760.
- 1442 84. Morgulis A, Gertz EM, Schaffer AA, Agarwala R: **A fast and symmetric DUST**
1443 **implementation to mask low-complexity DNA sequences.** *J Comput Biol* 2006,
1444 **13**(5):1028-1040.
- 1445 85. McKenna A, Hanna M, Banks E, Sivachenko A, Cibulskis K, Kernytzky A, Garimella K,
1446 Altshuler D, Gabriel S, Daly M *et al*: **The Genome Analysis Toolkit: a MapReduce**
1447 **framework for analyzing next-generation DNA sequencing data.** *Genome Res* 2010,
1448 **20**(9):1297-1303.
- 1449 86. Zhang Z, Li J, Zhao XQ, Wang J, Wong GK, Yu J: **KaKs_Calculator: calculating Ka and**
1450 **Ks through model selection and model averaging.** *Genomics Proteomics*
1451 *Bioinformatics* 2006, **4**(4):259-263.

- 1452 87. Li L, Stoeckert CJ, Jr., Roos DS: **OrthoMCL: identification of ortholog groups for**
 1453 **eukaryotic genomes.** *Genome Res* 2003, **13**(9):2178-2189.
 1454 88. Edgar RC: **MUSCLE: a multiple sequence alignment method with reduced time and**
 1455 **space complexity.** *BMC Bioinformatics* 2004, **5**:113.
 1456 89. Capella-Gutierrez S, Silla-Martinez JM, Gabaldon T: **trimAl: a tool for automated**
 1457 **alignment trimming in large-scale phylogenetic analyses.** *Bioinformatics* 2009,
 1458 **25**(15):1972-1973.
 1459 90. Stamatakis A: **RAxML version 8: a tool for phylogenetic analysis and post-analysis**
 1460 **of large phylogenies.** *Bioinformatics* 2014, **30**(9):1312-1313.
 1461 91. Larsson A: **AliView: a fast and lightweight alignment viewer and editor for large**
 1462 **datasets.** *Bioinformatics* 2014, **30**(22):3276-3278.

1463
 1464
 1465
 1466
 1467
 1468
 1469
 1470
 1471
 1472
 1473
 1474

Tables

Nuclear genome features	<i>P. vinckei vinckei</i> CY	<i>P. vinckei brucechwatti</i> DA	<i>P. vinckei lentum</i> DE	<i>P. vinckei petteri</i> CR	<i>P. vinckei subsp. EL</i>
Genome Size (Mb)	18.34	19.17	19.31	19.39	19.50
G+C content (%)	22.94	23.17	23.33	23.19	23.16
Gaps within assembly	0	0	7	0	11
Genes	5,042	5,238	5,249	5,310	5,307
Pseudogenes	19	40	29	36	36
<i>ema1</i>	7	20	19	15	21
<i>etramp</i>	12	12	11	13	12
<i>fam-a</i>	87	187	201	188	207
<i>fam-b</i>	28	38	41	40	44
<i>fam-c</i>	20	59	63	64	65
<i>fam-d</i>	6	13	27	21	21
<i>hdh</i>	7	9	12	13	14
<i>lpl</i>	25	23	24	23	17
<i>p235</i>	5	8	7	6	8
<i>pir</i>	178	209	210	272	247

1475

1476 **Table 1. Genome assembly characteristics of five *Plasmodium vinckei***
1477 **reference genomes.** AT-rich *P. vinckei* genomes are 19.2 to 19.5 megabasepairs
1478 (Mbps) long except for *Pv*CY which has a smaller genome size of 18.3 Mb, similar
1479 to *Plasmodium berghei*. PacBio long reads allowed for chromosomes to be
1480 assembled as gapless unitigs with a few exceptions. Number of genes include partial
1481 genes and pseudogenes. Copy numbers of the ten multigene families differ between
1482 the *P. vinckei* subspecies (*ema1*, erythrocyte membrane antigen 1, *etramp*, early
1483 transcribed membrane protein, *hdh*, haloacid dehalogenase-like hydrolase, *lpl*,
1484 lysophospholipases, *p235*, reticulocyte binding protein, *pir*, *Plasmodium* interspersed
1485 repeat protein).

1486

1487

1488 **Figure legends**

1489 **Figure 1. *Plasmodium vinckei* parasites and their phenotypic characteristics.**

1490 A) Rodent malaria parasite species and subspecies and the geographical sites in
1491 sub-Saharan Africa where from which they were isolated (modified from [1]).
1492 *Plasmodium vinckei* is the only RMP species to have been isolated from five different
1493 locations. Inset: To date, several RMP isolates have been sequenced (black) to aid
1494 research with rodent malaria models. Additional RMP isolates have been sequenced
1495 in this study (red) to cover all subspecies of *P. vinckei* and further subspecies of
1496 *Plasmodium chabaudi* and *Plasmodium yoelii*. B) Morphology of different life stages
1497 of *P. vinckei baforti* EL. R: Ring, ET: early trophozoite, LT: Late trophozoite, S:
1498 Schizont, MG: Male gametocyte, FG: Female gametocyte, O: oocyst and Sp:
1499 Sporozoite. *Plasmodium vinckei* trophozoites and gametocytes are morphologically

1500 distinct from other RMPs due to their rich haemozoin content (brown pigment). C)
1501 Parasitaemia of ten *P. vinckei* isolates (split into two graphs for clarity) during
1502 infections in mice (n=5) for a 20-day duration. † denotes host mortality. *Plasmodium*
1503 *vinckei* isolates show significant diversity in their virulence phenotypes.

1504

1505 **Figure 2. Structural variations and genotypic diversity among *Plasmodium***
1506 ***vinckei* parasites.** A) Chromosomal rearrangements in *P. vinckei* parasites.
1507 Pairwise synteny was assessed between the five *P. vinckei* subspecies and
1508 *Plasmodium berghei* (to represent the earliest common RMP ancestor). The 14
1509 chromosomes of different RMP genomes are arranged as a Circos plot and the
1510 ribbons (grey) between them denote regions of synteny. Three reciprocal
1511 translocation events (red) and one inversion (blue) accompany the separation of the
1512 different *P. vinckei* subspecies. A pan-*vinckei* reciprocal translocation between
1513 chromosomes VIII and X was observed between *P. vinckei* and other RMP
1514 genomes. Within the *P. vinckei* subspecies, two reciprocal translocations, between
1515 chromosomes V and XIII, and between chromosomes V and VI, separate
1516 *Plasmodium vinckei petteri* and *P. v. baforti* from the other three subspecies. A small
1517 inversion of ~100 kb region in chromosome 14 has occurred in *Pv*vCY alone. B)
1518 Maximum likelihood phylogeny of different RMP species with high-quality reference
1519 genomes based on protein alignment of 3,920 one-to-one orthologs (bootstrap
1520 values of each node are shown). Genomes of three human malaria species-
1521 *Plasmodium falciparum*, *Plasmodium vivax* and *Plasmodium knowlesi* were included
1522 in the analysis as outgroups. C) Maximum likelihood phylogenetic tree of all
1523 sequenced RMP isolates based on 1,010,956 high-quality SNPs (bootstrap values of
1524 each node are shown). There exists significant genotypic diversity among the *P.*

1525 *vinckei* isolates compared to the other RMPs. All *P. vinckei* subspecies have begun
1526 to diverge from their common ancestor well before sub-speciation events within
1527 *Plasmodium yoelii* and *Plasmodium chabaudi*. Genetic diversity within *P. v. petteri*
1528 and *P. v. baforti* isolates are similar to those observed within *P. yoelii* and *P.*
1529 *chabaudi* isolates while *P. v. lentum* and *P. v. brucechwatti* isolates have
1530 exceptionally high and low divergences respectively. Genes with significantly high
1531 Ka/Ks ratios in different subspecies-wise comparisons (as indicated by connector
1532 lines), the gene's Ka/Ks ratio averaged across all indicated *P. vinckei* comparisons
1533 and geographical origin of the isolates are shown.

1534

1535 **Figure 3. Sub-telomeric multigene family expansions in *Plasmodium vinckei***
1536 **parasites. A)**

1537 Violin plots show sub-telomeric multigene family size variations among RMPs and
1538 *Plasmodium falciparum*. The erythrocyte membrane antigen 1 and *fam-c* multigene
1539 families are expanded in the non-Katangan *P. vinckei* parasites (red). Apart from
1540 these families, multigene families have expanded in *P. vinckei* similar to that in
1541 *Plasmodium chabaudi*. The Katangan isolate *PvCY* (purple) has a smaller number
1542 of family members compared to non-Katangan isolates (orange) except for
1543 lysophospholipases, *p235* and *pir* gene families. B) Maximum Likelihood phylogeny
1544 of 99 *ema1* (top) and 328 *fam-c* (bottom) genes in RMPs. Branch nodes with good
1545 bootstrap support (> 70) are marked in red. The first coloured band denotes the
1546 RMP species to which the particular gene taxon belongs to. The heatmap denotes
1547 the relative gene expression among rings, trophozoite, schizont and gametocyte
1548 stages in the RMPs for which data are publicly available. Orange denotes high
1549 relative gene expression and white denotes low relative gene expression, while grey
1550 denotes lack of information. Gene expression was classified into three categories

1551 based on FPKM level distribution- High (black) denotes the top 25% of ranked FPKM
1552 of all expressed genes (FPKM > 256), Low (light grey) is the lower 25% of all
1553 expressed genes (FPKM < 32) and Medium level expression (grey; 32 < FPKM < 256).
1554 “P” denotes pseudogenes. Four *vinckei*-group (*P. chabaudi* and *P. vinckei*
1555 subspecies) specific clades (Clades I-IV; orange), two *vinckei*-specific clade (Clade
1556 IV and V; purple) and one non-Katangan-specific clade (Clade VI; blue) can be
1557 identified within *ema1* family with strong gene expression, maximal during ring
1558 stages. Rest of the family’s expansion within non-Katangan *P. vinckei* isolates are
1559 mainly pseudogenes with weak transcriptional evidence. The fam-c gene phylogeny
1560 shows the presence of four distinctly distal clades (A) with robust basal support (96-
1561 100). Of the four clades, two are pan-RMP (grey) and two are *vinckei* group-specific
1562 (orange), each consisting of fam-c genes positionally conserved across the member
1563 subspecies. Most members of these clades show medium to high gene expression
1564 during asexual blood stages. Other well-supported clades can be classified as either
1565 *berghei* group-specific (two; green), *vinckei* group-specific (two; orange), *P. vinckei* -
1566 specific (two; purple) or non-Katangan *P. vinckei* -specific clades (three; blue). There
1567 is evidence of significant species-specific expansion with striking examples in
1568 *Plasmodium yoelii* (i), *P. chabaudi* (ii) and in *P. v. brucechwatti* (iii).

1569

1570 **Figure 4. Phenotypic variation and genetics in *Plasmodium vinckei* parasites.**

1571 A) Schematic of isolate-specific genetic markers detected in clonal line of *PvsEL* X
1572 *PvsEH* cross progeny by Sanger sequencing. Genetic markers from both EH (red)
1573 and EL (blue) isolates were detected in the crossed progeny proving successful
1574 genetic crossing. B) Schematic of homologous recombination-mediated insertion of a
1575 *gfp-luciferase* cassette into the *p230p* locus in *P. vinckei* CY. C) GFP expression in

1576 different blood stages of *Pv*CY and luciferase expression of *Pv*CY oocysts in
1577 mosquito midgut.

1578

1579 **Additional files**

1580 **Additional file 1. Summary of rodent malaria parasite isolates used and DNA**
1581 **and RNA sequencing performed in this study.**

1582 **Additional file 2. Infection profiles of ten *Plasmodium vinckei* isolates.** Changes
1583 in parasitaemia, host RBC density and host weight during *P. vinckei* infections. Error
1584 bars show standard deviation of the readings within five biological replicates. †
1585 denotes host mortality.

1586 **Additional file 3. Daily readings of parasitaemia, host RBC density and host**
1587 **weight during infections of *Plasmodium vinckei* isolates.**

1588 **Additional file 4. Assembly statistics of *Plasmodium vinckei* mitochondrial and**
1589 **apicoplast genomes.**

1590 **Additional file 5. Chromosomal synteny breakpoints among *Plasmodium***
1591 ***vinckei* genomes.**

1592 **Additional file 6. 3,920 one-to-one orthologous group used for genome-wide**
1593 **protein alignment-based phylogeny.**

1594 **Additional file 7. Single nucleotide polymorphisms among RMP isolates and**
1595 **Ka/Ks ratios for various pair-wise comparisons of homologous protein-coding**
1596 **genes.**

1597 **Additional file 8. Copy number variations within multigene families and**
1598 **phylogenetic clade members.**

1599 **Additional file 9. Maximum Likelihood trees for ten RMP multigene families.**

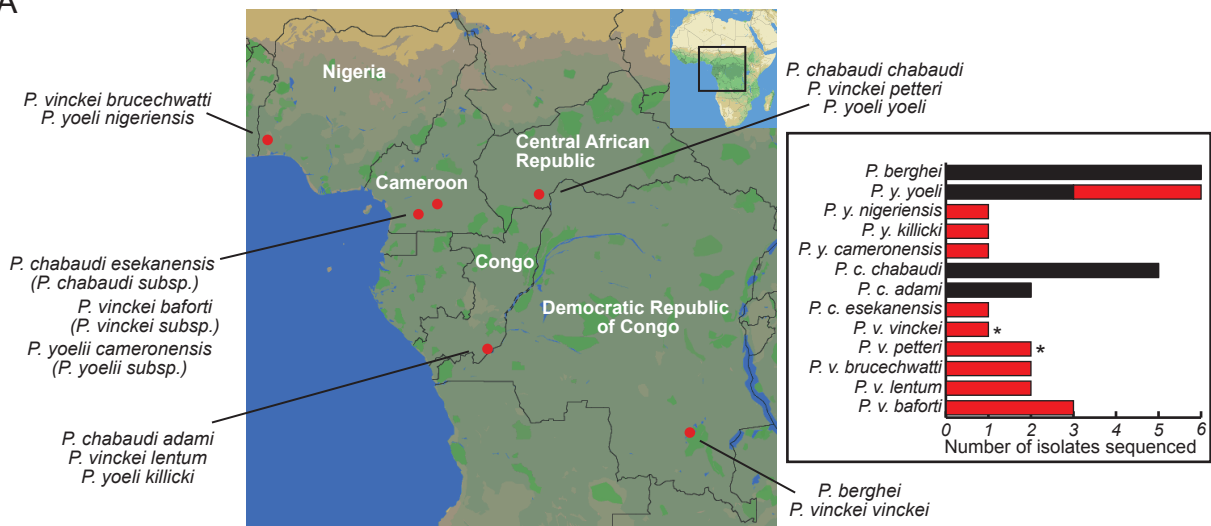
1600 **Additional file 10. Gene-wise RNA-seq FPKM values for *Plasmodium vinckei***
1601 ***petteri* CR, *P. v. lentum* DS (Rings, trophozoites and gametocyte stages), *P. v.***
1602 ***brucechwatti* DA and *P. v. baforti* EL (mixed blood stages).**

1603 **Additional file 11. Mosquito transmission and genetic cross experiments.**

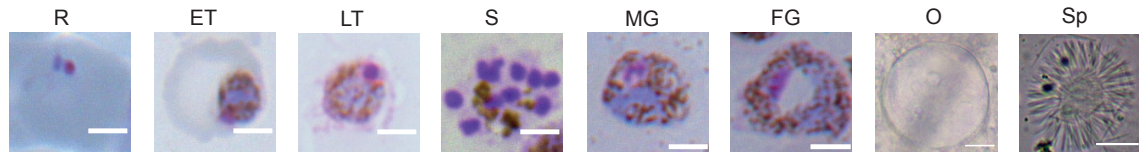
1604 **Additional file 12. A) Circos figure showing rearrangements among four RMP**
1605 **species B) Gene alignment of pseudogenised *ema1* genes.**

1606
1607

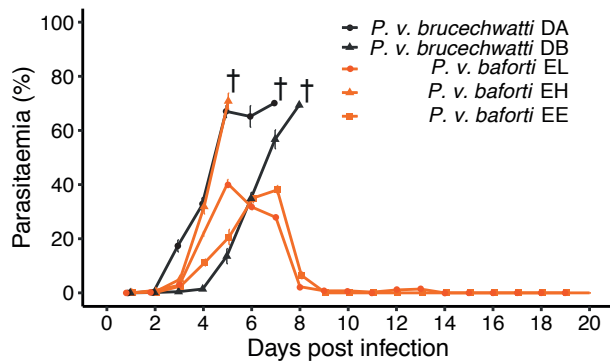
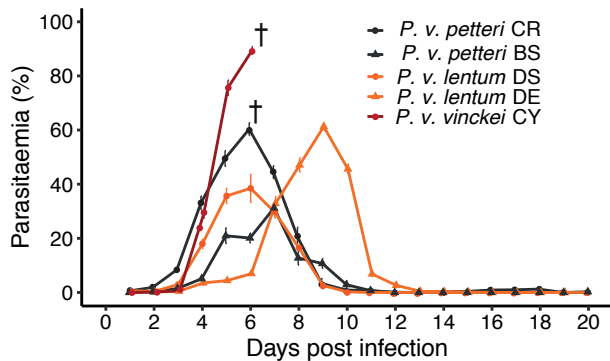
A

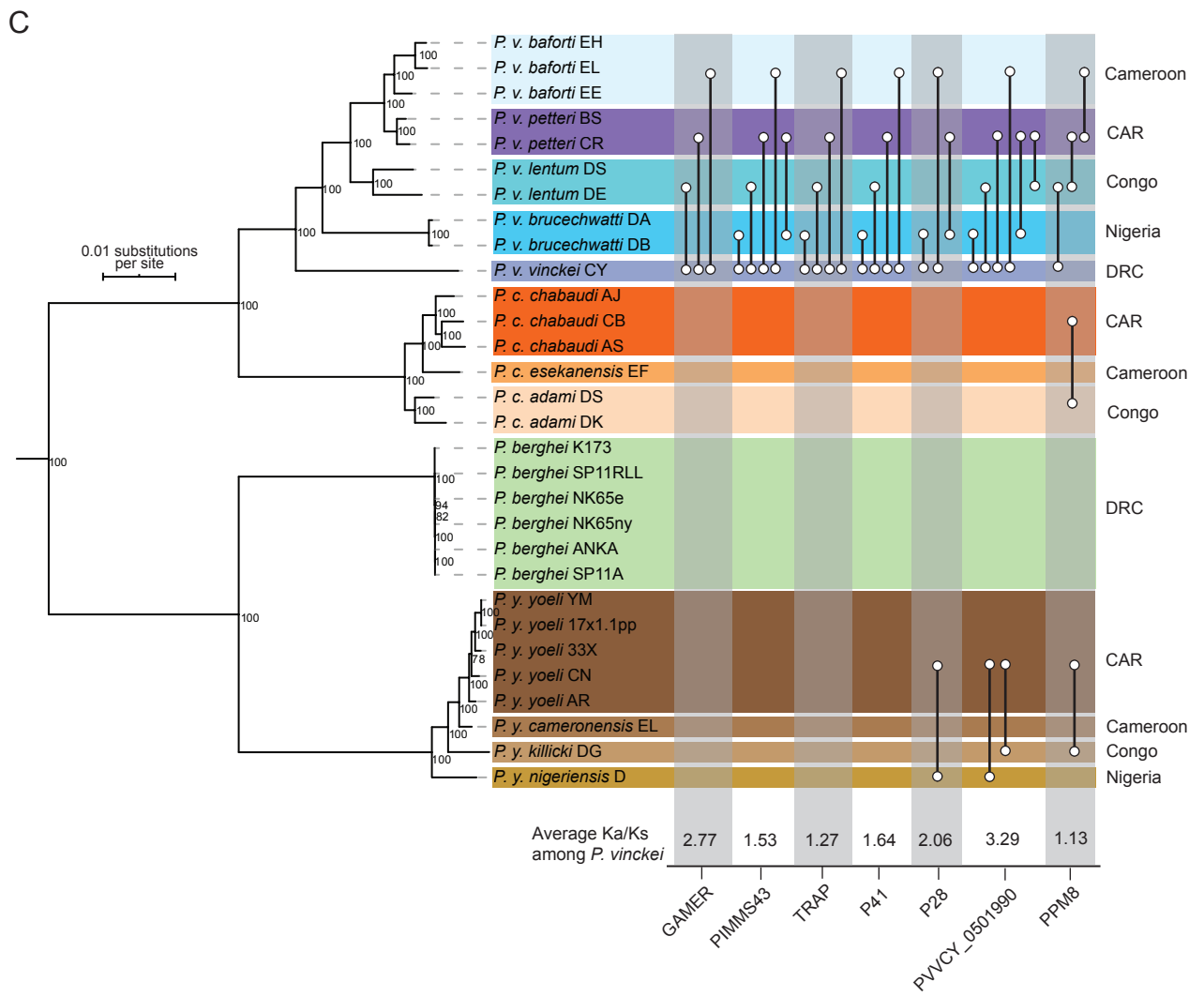
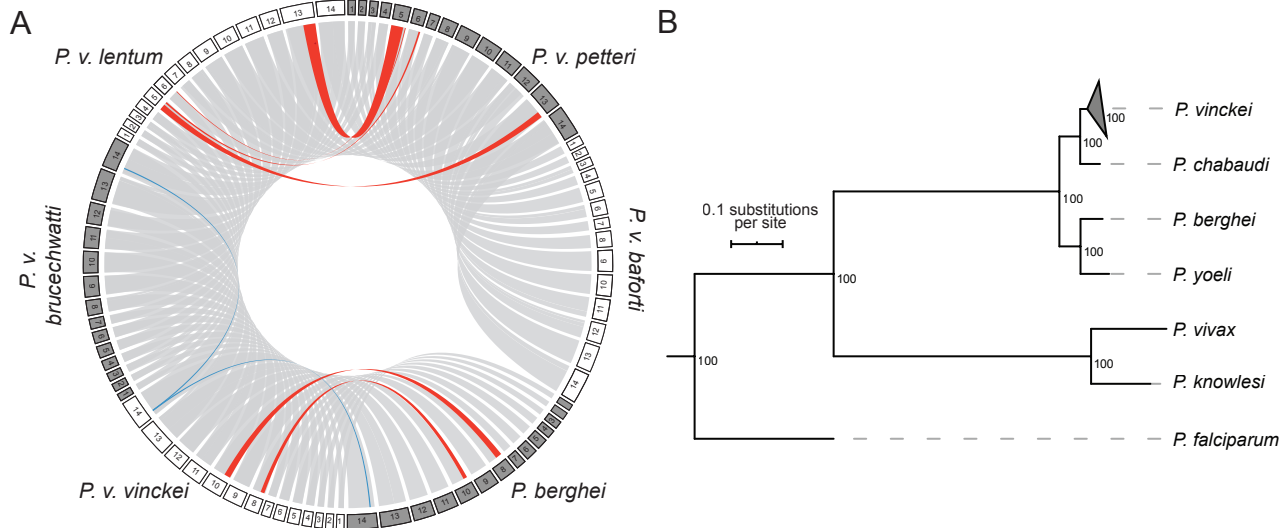


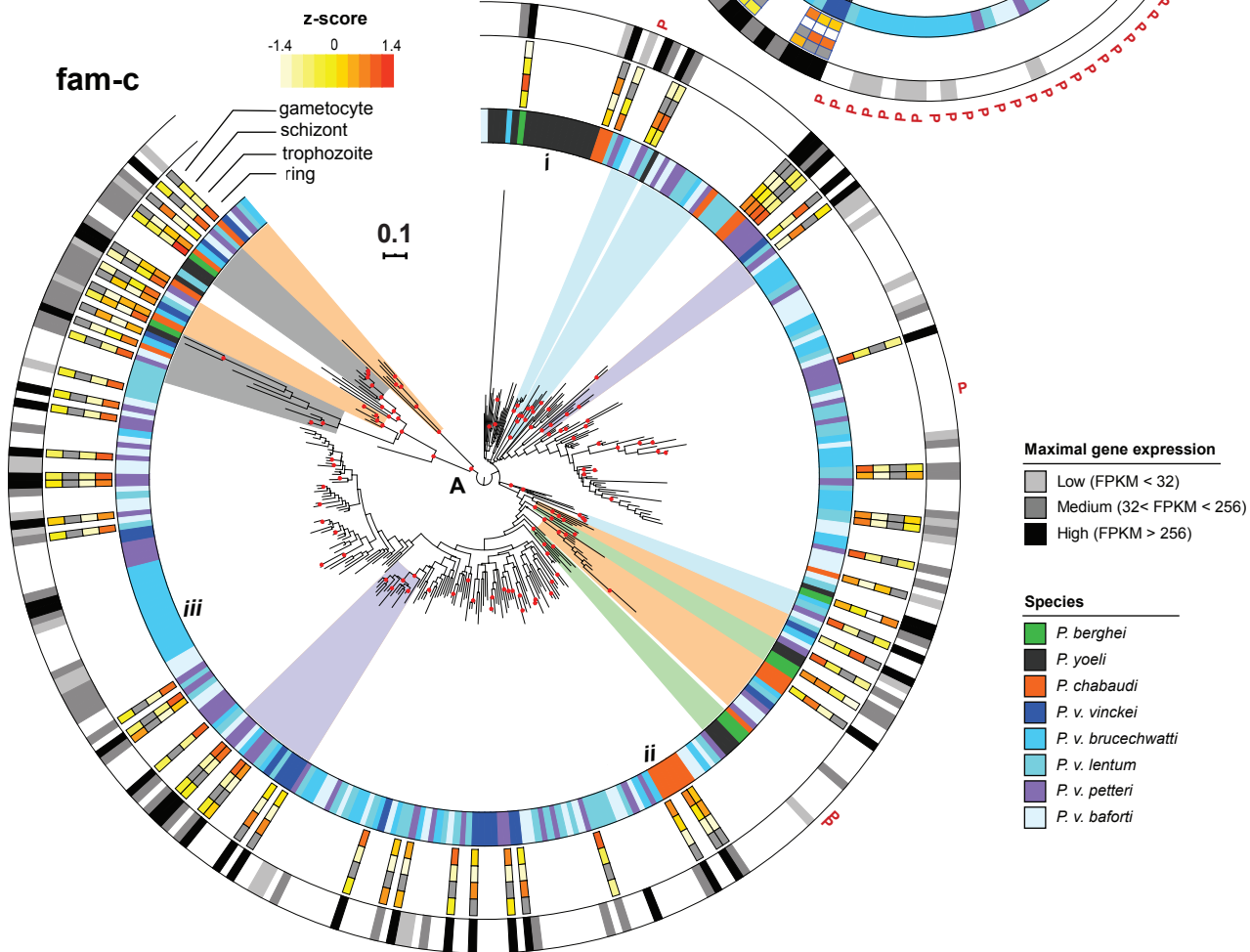
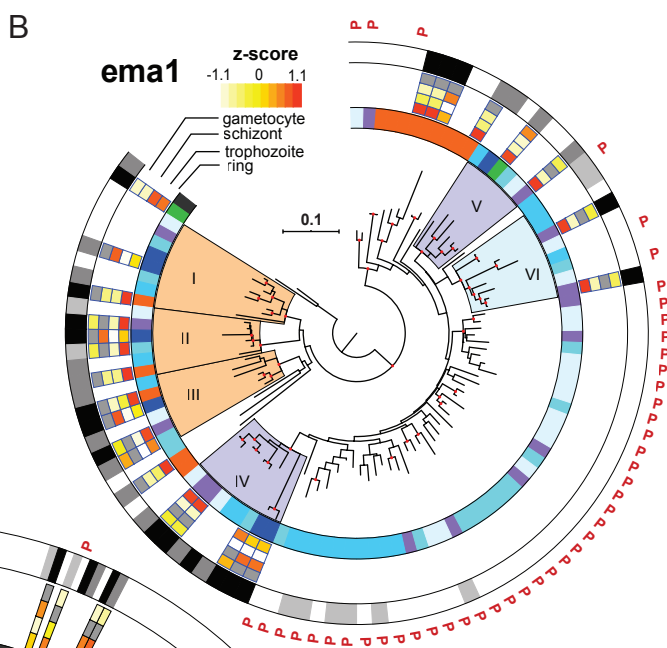
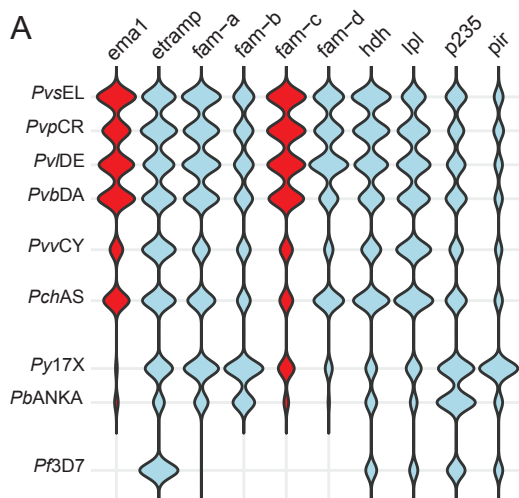
B



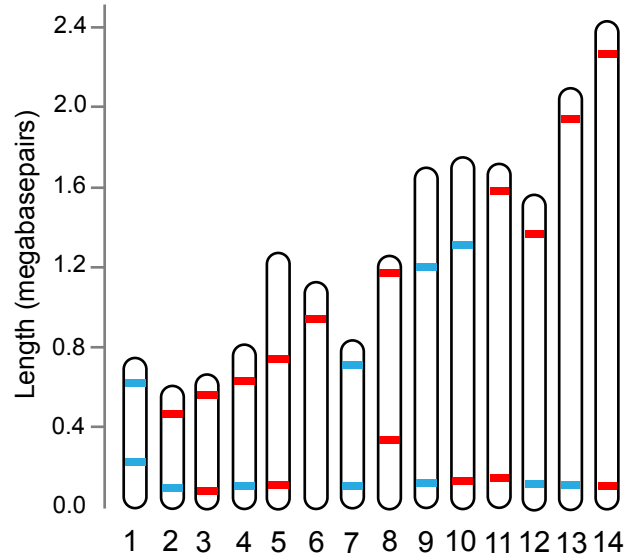
C



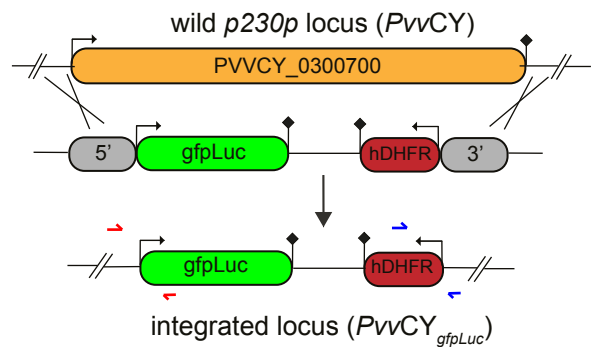




A ■ Gene derived from *P. vinckei baforti* EL
■ Gene derived from *P. vinckei baforti* EH



B



C

